Thiolutin is a direct inhibitor of RNA Polymerase II

Chenxi Qiu[1,6], Indranil Malik[1,7], Payal Arora[1,2], Amber J. Laperuta[3,8], Emily M. Pavlovic[4,9], Scott Ugochuckwu[5], Mandar Naik[1,10], Craig Kaplan[1,2]

[1] Department of Biochemistry and Biophysics, Texas A&M University, College Station, TX 77843, USA
[2] Department of Biological Sciences, University of Pittsburgh, Pittsburgh, PA 15260, USA
[3] Stevenson University, Stevenson, MD 21153, USA
[4] Earlham College, Richmond, IN 47374, USA
[5] Texas State University, San Marcos, TX 78666 USA
[6] Present Address: Department of Genetics, Harvard Medical School, Boston, MA 02115, USA
[7] Present Address: Department of Neurology, University of Michigan, Ann Arbor, MI 48109, USA
[8] Present Address: Department of Biological Sciences, Carnegie Mellon University, Pittsburgh, PA 15213, USA
[9] Present Address: University of Minnesota-Duluth, Duluth, MN 55812, USA
[10] Present Address: Department of Molecular Pharmacology, Physiology and Biotechnology, Brown University, Providence, RI 02912, USA

Abstract

Thiolutin is a well-known and long-used natural product transcription inhibitor with an unresolved mode of action. Recent studies have identified Zn^{2+}-chelation activity for both thiolutin and the related dithiolopyrrolone holomycin, with direct inhibition of RNA polymerases ruled out as a mode of action. However, negative results for direct transcription inhibition of RNA polymerases in recent studies are contradicted by previously observed thiolutin inhibition of extract fractions containing yeast RNA Polymerases I, II, and III. Here, we present chemical genetic and biochemical approaches to investigate the mode of action of thiolutin. We identify diverse classes of mutant that alter sensitivity to thiolutin. We functionally dissect the multidrug resistance and thioredoxin pathways controlling thiolutin sensitivity. We provide genetic evidence that thiolutin causes oxidation of thioredoxins *in vivo* and suggest that thiolutin both induces oxidative stress and alters Zn^{2+}, Cu^{2+} and Mn^{2+} homeostasis *in vivo*, recapitulating previously observed thiolutin interactions with Zn^{2+}. Finally, our results resolve contradictory biochemical results for thiolutin inhibition of transcription by direct demonstration of thiolutin inhibition of RNA polymerase II (Pol II) *in vitro*. Inhibitory activity requires both appropriate reduction of thiolutin and the presence of Mn^{2+}. Thio/Mn^{2+} inhibition is abrogated when template DNA is pre-bound to Pol II or when excess DTT is present, and renders Pol II pause prone in elongation if initiation is bypassed using a pre-formed Pol II elongation complex. Together, we propose that thiolutin directly inhibits Pol II transcription through a novel mechanism distinct from known transcription inhibitors.

Introduction

Thiolutin is a historically used transcription inhibitor with potentially multiple modes of action. Thiolutin one of a number of microbially produced dithiolopyrrolone compounds, holomycin being the most notable of this class, that feature an intra-molecular and redox-sensitive disulfide bond[1,2]. These compounds are thought to be pro-drugs whose anti-microbial action requires reduction of the intramolecular disulfide. Thiolutin has been shown to inhibit bacterial and eukaryotic transcription *in vivo* and has been used to study mRNA stability in multiple species[3-6]. However, the mode of action of thiolutin for transcription inhibition remains unclear and complicated (discussed below). In addition, thiolutin appears to affect multiple cellular pathways, including glucose metabolism, Hog/MAPK pathway signaling, P body formation, mRNA degradation, oxidative stress response, and proteasome activity[7-11].

Recent progress has suggested that both thiolutin and holomycin act as redox-sensitive Zn^{2+} chelators, providing an explanation for their diverse cellular effects[1,10,12,13]. It has been demonstrated *in vitro* that thiolutin and holomycin can be reduced by strong reductants such as DTT or TCEP[1,10] and that reduced thiolutin and holomycin can chelate Zn^{2+} [10,12]. The Zn^{2+} chelating activity explains multiple thiolutin induced phenotypes, including alteration of glucose metabolism and proteasome inhibition through Zn^{2+}-specific metalloproteins[7,10]. In addition, two observations suggest a possible mechanism for the thiolutin-induced expression of oxidative stress response genes[8]. First, thiolutin and holomycin appear to require reduction for their activity, and reduction of thiolutin could in turn oxidize the cellular reductant or reducing proteins[1,12]. Second, reduced holomycin can be spontaneously oxidized by molecular oxygen, suggesting that holomycin may be a redox cycling compound[14,15] and cause accumulation of reactive oxygen species (ROS). Whether thiolutin can act as a redox cycler has not yet been tested, and the cellular reductant(s) for thiolutin or holomycin remain unclear, because glutathione does not reduce holomycin *in vitro*[1]. Together, the Zn^{2+} chelating and redox activities are consistent with previously observed diversity in thiolutin-induced phenotypes, though transcription inhibition is not easily explained. Both thiolutin and holomycin have been observed to be inert against RNAPs under conditions where either should be able to chelate Zn^{2+}. Furthermore, it is not clear how Zn^{2+} chelation would be expected to inhibit transcription. In light of these negative results, transcription inhibition by dithiolopyrrolones was concluded to be a secondary outcome of inhibition of a distinct target, such as the proteasome. Thiolutin effects removal of zinc from Rpn11, an essential deubiquitinase required for proteasomal processing of ubiquitinated substrates[10,12].

There is extensive evidence for thiolutin inhibition of transcription *in vivo* in multiple species[16-18], though from *in vitro* studies it has been concluded that it inhibits prokaryotic and eukaryotic RNAPs differently. Thiolutin inhibited all three partially purified yeast RNAPs *in vitro*[19], but failed to inhibit all tested prokaryotic RNAPs *in vitro*[17,18,20]. Similar RNAP inhibition *in vivo* with lack of inhibition *in vitro* has been observed for holomycin[12,21]. The recently reported lack of thiolutin inhibition for all three fully purified yeast RNAPs has added further confusion[10]. Therefore, our current state of understanding is that thiolutin and holomycin do not appear to inhibit prokaryotic or fully purified eukaryotic RNAPs, suggesting indirect modes of *in vivo* transcription inhibition. However, without comprehensive assessment of the experimental parameters for different transcription assays, it seems difficult to rule out direct mechanisms of action for thiolutin on eukaryotic RNAPs, as recent work does not satisfactorily explain why thiolutin inhibited all three partially purified yeast RNA polymerases *in vitro*[19], and how thiolutin inhibited RNAPs prior to template addition, but did not inhibit the template DNA bound RNAPs[19]. This critical order-of-addition requirement for treatment prior to DNA addition is reminiscent of RNAP switch region

inhibitor behavior[22,23] and is consistent with inhibition of a specific and early step in transcription, in contrast to Zn^{2+} chelation.

We can imagine a number of possibilities to reconcile the existing data. First, thiolutin may target a secondary protein, which is present *in vivo* and in partially purified RNA polymerase fractions[19] but not others[10,18,20]. Second, as predicted[10,12], thiolutin may act as a prodrug that is activated *in vivo* and under the *in vitro* conditions of the early report[19] but not in assays used by others[10,18,20]. To further investigate the mode of action of thiolutin, we have undertaken multiple approaches to screen for thiolutin resistant and sensitive mutants, as similar studies have contributed to understanding of modes of actions of many compounds[24-26], including holomycin[12]. We identify a drug efflux pump functioning in thiolutin resistance and demonstrate that thiolutin treatment appears to induce oxidative stress. We propose that thiolutin likely induces the oxidative stress via oxidizing thioredoxins and possibly also redox-cycling. In addition, we confirm that reduced thiolutin directly interacts with Zn^{2+} *in vitro*, consistent with the recent reports on holomycin and thiolutin using different approaches[10,12]. We also suggest that thiolutin alters cellular Zn^{2+} homeostasis in yeast similar to holomycin's effects in *E.coli*[12].

Finally, we have revisited *in vitro* biochemical studies with thiolutin and Pol II. We find that thiolutin indeed inhibits Pol II but critically requires the presence of small amounts of Mn^{2+}, providing an explanation for disparate results across studies. First, DNA bound Pol II is resistant to thiolutin inhibition, recapitulating Tipper *et al*'s early studies[19]. Second, though thiolutin appears to inhibit a very early step in Pol II transcription, when initiation is bypassed by use of specific nucleic acid templates, thiolutin-treated Pol II exhibits pause-prone, slow elongation. Third, high DTT reverses the thiolutin inhibition, suggesting involvement of disulfide bond or redox sensitive covalent chemistry in inhibition. We find that thiolutin appears to block initiation *in vivo* immediately after treatment, consistent with Pol II inhibition *in vivo* being direct. We propose that thiolutin inhibits Pol II transcription directly through a novel mechanism distinct from known Pol II transcription inhibitors.

Results

Thiolutin or reduced thiolutin alone fail to inhibit fully purified Pol II in vitro

Recent publications suggest that thiolutin does not directly inhibit Pol II, in contrast to classic in vitro transcription experiments demonstrating thiolutin inhibition of partially purified yeast extract fractions containing Pol I, II, or III[19]. We set out to understand this discrepancy by first examining thiolutin inhibition of purified Pol II. Given that thiolutin and holomycin activities could be sensitive to reduction of the disulfide bond by DTT[1,10,12] (Figure 1A), we removed DTT from the in vitro transcription reaction and performed the thiolutin treatment with or without molar equivalents of DTT (Figure 1B). Under buffer conditions employed here, we failed to observe thiolutin inhibition of Pol II, with DTT having no effect (Figure 1B). While these results are consistent with assertions that thiolutin does not directly target Pol II, they might similarly be explained by the absence of a cofactor or subtleties in experimental conditions between in vitro assays. We therefore set out to screen for potential co-factors and these biochemical assays are revisited later.

Three independent genetic screens for thiolutin resistant and sensitive mutants

To gain insights into factors controlling the cellular response to thiolutin, we performed three independent genetic screens for modifiers of thiolutin sensitivity (Figure 2A, Figure S1A). First, we performed a conventional forward genetic screen for thiolutin resistant mutants through UV mutagenesis followed by thiolutin resistance selection. The causal mutations for thiolutin resistance were identified by bulk segregant analysis and whole genome sequencing[27] (Figure S1A). Second, we screened a yeast Variomics library for individual thiolutin resistant

candidates[28]. The variomics library contains possibly random mutations for almost all yeast genes cloned into a CEN based plasmid and expressed in strains with the relevant endogenous gene deleted. The CEN based plasmid is known to replicate 1-2 copies in cells and could result in increased dosage of the gene[29]. Mutants from the forward genetics screen or reproducibly isolated from the manual Variomics screens were re-tested for resistance (Figure S1B, Table S1, S2). Third, we performed a set of high-throughput screens using both pooled Variomics and deletion libraries using barcode-sequencing (Bar-seq)[24,25] (Figure 2A, Material and Methods), where the thiolutin resistant and sensitive mutants were identified by quantifying changes of mutant-linked DNA barcode frequency under the thiolutin treated versus control conditions[25,30]. Overall, our data exhibited excellent reproducibility (Figure S2) and revealed valuable common and distinct features between Variomics (putative gain-of-function (GOF) and loss-of-function (LOF) mutants combined) and deletion (LOF mutants) libraries (see Material and Methods). We have revealed contribution of multidrug resistance (Figs S1B-E, S3), oxidative stress response (Figs S1F-G, S5), multiple divalent metal homeostasis/trafficking pathways (Figs 2,3,S7, S8) as well as the proteasome to thiolutin resistance (Fig S6), and we have further genetically dissected a subset of these pathways. These data collectively support that reduction and manganese appear to contribute to the thiolutin inhibitory activity, supporting a model that reduction and manganese are both required for thiolutin inhibition of Pol II in vitro, tested in subsequent biochemical experiments (Figs 4,5). Each of these pathways is discussed below.

Functional dissection of the multidrug resistance (MDR) and oxidative stress response (OSR) pathways in response to thiolutin

We identified thiolutin resistant strains harboring mutations in MDR and OSR genes from all three genetic screens. These results are perhaps not surprising given that yeast has well characterized MDR pathways that sense and pump out the toxic small molecules as a self-protection mechanism, or given the recent reports that thiolutin and holomycin activities require reduction in vitro[10,12]. Reduction of thiolutin may itself oxidize cellular proteins and cause oxidative stress. In addition, it has been reported that reduced holomycin may act as a redox cycler, which could possibly generate ROS. Consistent with redox activity, thiolutin appeared to induce expression of several OSR genes[8]. However, it has not been examined how thiolutin interacts with either MDR or OSR pathways. In light of our isolated thiolutin resistant mutants, we functionally dissected control of thiolutin sensitivity by these pathways. From both manual Variomics and forward genetic screens, we isolated multiple mutants in *YAP1* and *YRR1*, encoding transcription factors that have been implicated in OSR and MDR or MDR, respectively (Figure S1C). In addition, we also isolated mutants in the MDR efflux pump gene *SNQ2* from the manual Variomics screen. Finally, from high-throughput Bar-seq screens, we identified distinct thiolutin resistance and sensitivity in additional mutants linked to MDR transcription factors or efflux pumps (Figure 2B). Several lines of evidence suggested that the isolated thiolutin resistant MDR mutants were GOF mutations. First, isolated *yap1* mutants showed clustering of mutations in regions encoding the C-terminus, where a variety of mutants are known to cause GOF[31-35]. Second, isolated MDR mutants from the manual Variomics screen were dominant or functioned through increased dosage (overexpression) (Figure S3). Third, in Bar-seq screens, we found Variomics mutants in several MDR genes (*YAP1, YRR1, SNQ2*) conferred thiolutin resistance whereas deletion of the same genes either conferred sensitivity or had no strong effect (Figure 2B), consistent with these MDR Variomics mutants being different from the gene deletion mutants (complete LOF).

In order to better understand the nature of identified MDR mutants from variomics and forward genetics, we constructed a series of MDR gene deletion mutants and tested their sensitivity to thiolutin (Figure S1D). We found that none of the tested deletion mutants was thiolutin resistant (Figure S1D). The lack of resistance for all the tested MDR deletion strains is consistent with the

isolated thiolutin resistant MDR mutants from Variomics and forward genetics screens increasing MDR activity. In addition, *pdr1*Δ and *snq2*Δ conferred hypersensitivity to thiolutin (Figure S1D), consistent with the Pdr1 and Snq2 functions in promoting thiolutin resistance for WT strains. Together, we conclude that the MDR transcription factor Pdr1 is the major transcription factor efflux of thiolutin from the cell, whereas neither Yrr1 nor Yap1 appears to promote baseline resistance, given that *yap1*Δ and *yrr1*Δ do not confer thiolutin hypersensitivity. However, increased Yap1 or Yrr1 activities through mutations or dosage may increase efflux pump expression to promote thiolutin resistance, through their known linkage to many multidrug efflux pumps[36-38].

Holomycin did not inhibit yeast cell growth at low concentration[21], and we recapitulated these observations (Figure S4A). Given that structurally similar compounds may have different cell permeability and efflux efficiency, we asked whether the same set of MDR deletion strains conferred sensitivity to holomycin but failed to observe any (Figure S4A). This observation suggests the lack of holomycin sensitivity may not be due to selective efficiency of drug efflux, although we cannot rule out the possibility that thiolutin and holomycin may be transported by different efflux pumps.

In addition to MDR pathways, we also identified thiolutin-modulating mutations in OSR-related genes, including *YAP1* (discussed above) and genes in the thioredoxin pathway. Thioredoxins are a series of small anti-oxidant proteins that primarily function in reducing specific cysteines in client proteins (reviewed in [39] and references therein), and in turn are themselves reduced by thioredoxin reductases (Figure S1F). In yeast, there are two thioredoxin reductases (cytoplasmic Trr1 and mitochondrial Trr2) and three thioredoxins (cytoplasmic Trx1, Trx2; mitochondrial Trx3) (Figure S1F). Mutants in *TRR1* were reproducibly isolated from our manual Variomics screen (Figure S1B,E; Table S1). In addition, *TRR1** and *TRX1** plasmid bearing were resistant to thiolutin from high-throughput screening of Variomics but not deletion libraries (Figures 2B), suggesting that *TRR1** and *TRX1** plasmids in the Variomics library could be GOF due to specific mutation or increased dosage of the plasmid.

TRR1 was found to be essential in large scale gene deletion analysis[40] but nonessential in classical genetic experiments[41-45]. To understand the nature of *TRR1* function in thiolutin resistance/sensitivity, we constructed a *trr1*Δ strain to directly test its thiolutin sensitivity (Figure S1G). Interestingly, *trr1*Δ conferred hypersensitivity to thiolutin (Figure S1G), consistent with Trr1 activity antagonizing thiolutin and specific *TRR1** mutants or increased Trr1 dosage enhancing this antagonism. The Trr1 function in antagonizing thiolutin also suggests that our isolated *yap1* alleles could confer thiolutin resistance through promoting *TRR1* expression, among other mechanisms.

We conceive of *trr1*Δ hypersensitivity to thiolutin in two ways. It could be due to loss of Trr1 function in directly counteracting thiolutin activity or the accumulation of oxidized thioredoxins, or both. The observed *TRX1**-linked thiolutin resistance in high-throughput Variomics screens suggested critical functions of thioredoxin(s) in thiolutin resistance downstream of *TRR1*. Therefore, we examined thioredoxin deletions directly for thiolutin resistance. We found that the *trx1*Δ, *trx2*Δ, or *trx1*Δ *trx2*Δ mutants did not confer thiolutin sensitivity (Figure S1G). In contrast, *trx1*Δ *trx2*Δ conferred thiolutin resistance, and further, suppressed thiolutin hypersensitivity of *trr1*Δ (Figure S1G), consistent with the hypothesis that *trr1*Δ hypersensitivity to thiolutin is due to accumulation of oxidized thioredoxins. The observed *trx1*Δ *trx2*Δ thiolutin resistance reveals critical requirement of Trx1 and Trx2 for thiolutin activity and suggests that Trx1 and Trx2 may function either directly or indirectly in thiolutin reduction. However, further experiments are needed to demonstrate the direct thiolutin reduction by Trx1 or Trx2.

Thiolutin resistance conferred by *yap1* alleles and thioredoxin mutants suggests possible connections to OSR. Therefore, we set to test the roles of two additional OSR genes, *TSA1*, encoding a thioredoxin peroxidase, and *SOD1*, encoding a cytosolic copper-zinc superoxide dismutase, in thiolutin resistance. Interestingly, *sod1*Δ, but not *tsa1*Δ, conferred hypersensitivity to thiolutin (Figure S1G). Given that holomycin is a known redox cycler, we asked if simple addition of H2O2 could mimic the thiolutin effect in tested thioredoxin and OSR gene deletion mutants (Figure S1G). Thiolutin sensitivities in tested strains were distinct from H2O2 sensitivities, suggesting distinct effects on cellular function. Finally, we tested if yeast could be sensitized to holomycin by the same set of mutants (Figure S4). Interestingly, *trr1*Δ and *sod1*Δ were slightly sensitive to 10 µg/mL holomycin (Figure S4), suggesting that the induction of oxidative stress could be general property of dithiolopyrrolone compounds and that yeast are at least somewhat permeable to holomycin.

Thiolutin induces apparent oxidative stress

Multiple lines of evidence presented above indicated that thiolutin may induce oxidative stress and increased Yap1 function may promote thiolutin resistance. Yap1 functions by sensing the cellular oxidants through its C-terminal cysteines, causing it to translocate into the nucleus and up-regulating a series of OSR genes to counteract the cellular oxidants upon oxidative stress[31-35]. Therefore, nuclear localization of Yap1 is in general a sign of increased Yap1 function and OSR[31,34,35]. To test whether thiolutin treatment caused nuclear translocation of Yap1, we fused *YAP1* to sequence encoding EGFP on the Yap1 C-terminus, and monitored Yap1::EGFP localization after thiolutin treatment. Thiolutin indeed induced Yap1::EGFP nuclear localization, consistent with induction of oxidative stress, although the thiolutin induced Yap1::EGFP nuclear translocation appeared to be slower and weaker than that induced by H2O2 (Figure S5A). In addition, thiolutin depleted total glutathione within an hour of treatment (Figure S5B). However, thiolutin depleted both active GSH and GSSG, a behavior similar to glutathione synthesis defective mutants but distinct from several well-known oxidants such as H2O2 and menadione[46-48]. In contrast, holomycin did not have a clear effect on Yap1 localization or cellular glutathione levels (Figure S5A), consistent with the lack of growth inhibition by holomycin and the distinct activities or trafficking in yeast between the two structurally similar compounds.

Previous studies suggested that the reduced holomycin was spontaneously re-oxidized when exposed to air[1], consistent with the behavior of redox-cycling compounds. To test if thiolutin exhibited similar behavior, we monitored thiolutin reduction and re-oxidation by its unique UV absorbance due to the conjugated ene-dithiol groups (Figure S5C), as with the recent reports[1,10,12]. Thiolutin could be reduced by DTT or TCEP, but not glutathione (Figure S5C), consistent with the behavior of holomycin[1]. Reduced thiolutin could be also re-oxidized (Figure S5D), suggesting that thiolutin can act as a redox-cycler, similar to holomycin. Together, thiolutin induced the Yap1 nuclear accumulation and hypersensitivity of *sod1*Δ and *trr1*Δ mutant in vivo and appeared to be a redox cycler in vitro, consistent with the induction of oxidative stress. However, we did not find direct evidence of glutathione oxidation, suggesting that the nature of the in vivo reductant remains unclear.

DNA damage can be a consequence of redox-cycling and can lead to transcription inhibition and cytotoxicity[49,50]. We asked if thiolutin treatment could cause DNA damage or decrease viability. We did not observe an increase in mutation rate as measured by resistance to canavanine, consistent with little or no effect on DNA damage rates, nor did we observe a viability defect (Figure S5E, F). The lack of viability defect is consistent with an early report showing that thiolutin inhibition was reversible after several hours' treatment[51]. Together, we

suggest that thiolutin is a redox cycler in vitro and possibly also in vivo but does not appear to inhibit transcription through widespread DNA damage.

Additional cellular pathways are involved in thiolutin resistance

The high-throughput screens of pooled yeast Variomics and Deletion libraries, compared to conventional forward genetics and manual Variomics screens, revealed several additional pathways in thiolutin resistance (Figure 2B). We isolated mutants involved in the metal homeostasis, SWI/SNF complex, proteasome, ribosomal RNA biogenesis, and small ribosomal subunits (Figure 2B). Many observations from the Variomics screens were already independently confirmed from two conventional screens, direct deletion analyses or existing literature (Figure S1, Table S2). For example, deletion of SWI/SNF complex subunits *SWI3* and *SNF12* have been shown to confer sensitivity to a variety of divalent metals[52-56], consistent with thiolutin perturbation of metal homeostasis (discussed more below). We further constructed 9 haploid (for non-essential genes) or heterozygous (for essential genes) deletion mutants to validate the observation from the bar-seq screens of the deletion libraries. We validated the observations in 7 (out of 9) mutants, including one resistant and one sensitive mutant from the non-essential deletion pool, and 5 resistant mutants from essential heterozygous diploid pool (Figure S6). Among them, we validated the observed thiolutin resistance conferred by three heterozygous deletion strains in proteasome subunits (*PRE10/pre10*Δ, *PUP1/pup1*Δ, *RPN5/rpn5*Δ) (Figure S6).

The reconstructed strains validated the surprising but clear observation that heterozygous deletion mutants in proteasome subunits universally conferred thiolutin resistance (Figure S6). This is surprising because thiolutin was recently demonstrated to be a proteasome inhibitor through Zn^{2+} chelation, and heterozygous proteasome subunit deletion mutants presumably may lead to reduced proteasome activity and would be expected to confer sensitivity to proteasome inhibitors. Interestingly, two recent reports observed similar paradoxical resistance to proteasome inhibitors in yeast strains and human cell lines with decreased level of the regulatory 19S proteasome subunits[57,58]. In yeast and human, the fully assembled 26S proteasome consists of a 20S catalytic core and a 19S regulatory complex. It was demonstrated that decrease or transient inhibition of 19S proteasome subunits may in turn induce the level and activity of partially assembled 20S proteasome instead of the fully assembled 26S proteasome[58], resulting in a net increase of proteasome function. It was also recently suggested that specific reduced expression of 19S proteasome subunits induced an altered cellular state and altered the global transcriptome in response to proteasome inhibitors[59]. However, our observation is distinct, because we observed decreases in both 19S and 20S proteasome subunits conferred thiolutin resistance. Whether the proteasome has increased level and activity in these strains has yet to be tested.

Thiolutin alters divalent metal homeostasis

The recent detection of direct Zn^{2+} chelation activity of reduced thiolutin and holomycin explains multiple thiolutin-induced phenotypes, such as inhibition of proteasome and glucose metabolism[7,10,12]. From the high-throughput screens, we observed distinct thiolutin resistance or sensitivity linked to diverse Zn^{2+} trafficking genes, including those encoding the master transcription regulator Zap1 and various Zn^{2+} transporters Zrt1, Zrt2, Zrc1 and Cot1 (Figure 2B). Variomics strains linked to *ZAP1, ZRT1, ZRT2, ZRC1* and *COT1* conferred thiolutin resistance whereas deletion mutants were either not resistant (*zrt1*Δ, *zrc1*Δ, *cot1*Δ) or hypersensitive (*zap1*Δ and *zrt2*Δ) (Figure 2B), suggesting that these Variomics mutants could be gain-of-function or dosage modifiers in thiolutin resistance.

We first constructed a *zap1*Δ strain and tested its sensitivity to thiolutin (Figure 3A). *zap1*Δ confers hypersensitivity to thiolutin, consistent with Zap1 function in cellular resistance to thiolutin and thiolutin alteration of Zn^{2+} homeostasis in vivo. Notably, *zap1*Δ also conferred hypersensitivity to holomycin (Figure S7A). This observation is consistent with the reports that altering zinc homeostasis is a conserved mechanism among dithiolopyrrolones, and that holomycin could deplete cellular Zn^{2+} or access other essential targets in yeast if zinc homeostasis were perturbed, and suggesting that yeast resistance to holomycin may be partially explained by efficient transportation of Zn^{2+} that counteract active reduced holomycin. To rule out if *zap1*Δ hypersensitivity to thiolutin and holomycin is due to zinc deficiency-induced oxidative stress[60-63], *zap1*Δ hyper-sensitivity to thiolutin and holomycin was much stronger than that to H2O2, suggesting the *zap1*Δ hypersensitivity to thiolutin and holomycin is distinct from general oxidative stress exacerbation and is likely Zn^{2+} homeostasis defects. Finally, Zn^{2+} supplementation at high concentration partially suppressed the thiolutin inhibition (Figure S7C). The lack of full suppression suggests that there may be other thiolutin-mediated defects in addition to Zn^{2+} chelation, although we cannot rule out that inefficient Zn^{2+} trafficking limits effective Zn^{2+} supplementation in the cell.

In addition to Zn^{2+} homeostasis mutants, we observed a number of genes involved in Mn^{2+} trafficking (*PMR1, CCC2, VPS17, VPS25, SMF2*) linked to thiolutin resistance (Figure 2B). Interestingly, *PMR1* is a high affinity Ca^{2+} and Mn^{2+} ATPase that is required for Ca^{2+} and Mn^{2+} transport to Golgi and subsequent export[64,65]. *pmr1*Δ has been shown to increase intracellular Mn^{2+} level and appeared to confer thiolutin sensitivity (Figure 2B), which we confirmed by reconstructing *pmr1*Δ mutant and plate phenotyping (Figure 3B, Figure S8A). In contrast, deletion of *SMF2*, a transporter for importing divalent metals including Mn^{2+}, has been shown to cause intracellular Mn^{2+} depletion and conferred slight but consistent thiolutin resistance (Figure S8A). Together, the intracellular level of Mn^{2+} appeared to be positively correlated with thiolutin hypersensitivity, suggesting a mechanism distinct from Zn^{2+}, where Zn^{2+} supplementation confers partial thiolutin resistance (Figure S7C). To rule out the possibility that this altered thiolutin sensitivity is due to indirect effect from interference of other divalent metals, we phenotyped wild-type yeast strain in the presence of thiolutin and Mn^{2+} supplementation. Indeed, we observed that Mn^{2+} dose dependently exacerbated thiolutin sensitivity in wild-type yeast, supporting the synergy between Mn^{2+} and thiolutin in vivo.

In addition to *pmr1*Δ, we also confirmed the thiolutin hypersensitivity of *vps17*Δ and *vps25*Δ (Figure S8A). Vps17 and Vps25 are two vacuolar protein sorting genes and have been implicated in degradation of the Mn^{2+}-importing protein Smf1, thus possibly causing intracellular accumulation of Mn^{2+} and conferring thiolutin hypersensitivity. However, *vps17*Δ and *vps25*Δ were not more sensitive to Mn^{2+} than WT in our strain background (Figure S8B) and we found that *smf1*Δ did not suppress the hypersensitivity conferred by *vps17*Δ or *vps25*Δ (Figure S8A), suggesting that other mechanisms may be involved in these two Vps mutants.

Given the contrasting Zn^{2+} and Mn^{2+} modulation of thiolutin activity, we tested whether reduced thiolutin chelates Mn^{2+} and Cu^{2+}, while also confirming Zn^{2+} chelation. Consistent with the two recent reports, Zn^{2+} caused a distinct UV shift of reduced thiolutin from ~340nm to ~370nm but did not change the UV spectra of non-reduced thiolutin (Figure 3D, Figure S8C). In addition, we found that Mn^{2+} and Cu^{2+} can also interact with reduced but not non-reduced thiolutin, in a manner likely similar to Zn^{2+} binding (Figure 3D). Consistently, 1H-NMR experiments confirmed that DTT caused chemical shifts consistent with reduction of the ene-disulfide in thiolutin, and further chemical shifts caused by diamagnetic Zn^{2+} and selective broadening caused by paramagnetic Mn^{2+} were consistent with interactions between the divalent metals and the

thiolutin sulfhydryls (Figure S8, D and E). In contrast, Mg^{2+} did not bind to reduced thiolutin, distinct from the other tested metals (Figure 3D).

Thiolutin, when activated by DTT and Mn^{2+}, directly inhibits Pol II in vitro

Despite the progress in understanding thiolutin induced cellular phenotypes, whether and how thiolutin directly inhibits yeast Pol II in vitro remained unresolved. Multiple lines of evidence suggest possible involvement of divalent metals in this process. First, the co-clustering of thiolutin and bathophenanthroline induced phenotypic profiles suggests similar modes of action (Figure 2C). Bathophenanthroline is highly similar to a well-known transcription inhibitor 1,10-phenanthroline (Figure S9), which was suggested to require Cu^{2+} for direct transcription inhibition in vitro[66,67], though these compounds may have similar activities because they are also well-known Zn^{2+} chelators[68]. Second, the direct interaction between reduced thiolutin and Zn^{2+} (or Mn^{2+}, Cu^{2+}) suggests the possibility that thiolutin may function with metal co-factors.

Many divalent metals inhibit RNAP activity (e.g. Pb^{2+}, Zn^{2+}, Cu^{2+}, Be^{2+}, Cd^{2+}, Ca^{2+})[69], and additionally are tightly controlled in cells due to toxicity (*e.g.* Fe^{2+}, Co^{2+}), so are unlikely to participate in possible Pol II inhibition by thiolutin. Mn^{2+} does not inhibit but instead increases the activity of multiple RNA polymerases (including Pol II)[69]. In addition, Mn^{2+} is readily available in yeast cells (0.04-2mM depending on the type of measurement and genetically shown to be at levels that likely can alter Pol II activity in vivo)[70-74] at a relevant range to the reported thiolutin inhibitory concentration (~20μM in [19]). We note that in the original Tipper observations, their transcription buffer contained 1.6 mM Mn^{2+} as many classical transcription buffers included both Mn^{2+} and Mg^{2+} to maximize observed activity. In contrast, most other reports did not report Mn^{2+} in buffers[12,17,20,21] (One report appears to have a high concentration Mn^{2+} (10 mM) and possibly also reductant[18]). Therefore, we set out to test whether Mn^{2+} might participate in thiolutin-mediated inhibition of Pol II. Remarkably, Mn^{2+} addition to reduced thiolutin potently inhibited purified Pol II activity (Figure 4A), in sharp contrast to the activation of Pol II activity caused by Mn^{2+} by itself in the absence of reduced thiolutin. Our observation is consistent with the known stimulation of RNAPs by Mn^{2+} [69,75], but also suggests a potent Pol II inhibition by Mn^{2+} activated reduced thiolutin (hereafter termed as Thio/Mn^{2+}) (Figure 4A). Quantification of thiolutin inhibition at multiple concentrations and for controls leaving out specific components are shown in Figure S10.

We next designed a series of experiments to investigate properties of the inhibited Pol II and nature of the inhibitory species. We first tested if order-of-addition among Pol II, DNA and Thio/Mn^{2+} is critical for the inhibition, since order-of-addition is often informative on the mode of transcription inhibition, especially given the observation of Tipper *et al* that order-of-addition was critical for thiolutin inhibition in that study. Consistent with the early observation, we found that the template binding protects Pol II from the Thio/Mn^{2+} inhibition (Figure 4B). Template protection of Pol II suggests Thio/Mn^{2+} inhibits Pol II DNA interaction or similarly early step in transcription, consistent with the behavior of transcription initiation inhibitor. Therefore, we tested if Thio/Mn^{2+} affected Pol II elongation on a transcription bubble template using an RNA primer, where transcription initiation is bypassed. Surprisingly, Thio/Mn^{2+} altered, but did not block Pol II transcription elongation, inducing a highly pause prone Pol II elongation mode (Figure 4C, right panel). This was unexpected because most specific initiation inhibitors do not cause elongation defects, and DNA binding does not protect RNAPs from elongation inhibitors by their very nature. In addition, pre-assembled transcription elongation complexes were also resistant to Thio/Mn^{2+} (Figure 4C, middle panel), validating the critical order-of-addition in the non-specific transcription assay (Figure 4B). Thio/Mn^{2+} inhibited Pol II was pause-prone and appeared to irreversibly arrest at specific template positions (Figure 4C).

Whether thiolutin inhibits transcription initiation or elongation in vivo is unclear[16,20]. In light of our in vitro results, we tested thiolutin mediated Pol II transcription inhibition in vivo, by monitoring Pol II occupancy on a long gene, *YLR454W*. We observed a specific decrease of Pol II occupancy on the 5' end of the gene within the first 2 minutes, consistent with immediate transcription initiation inhibition after thiolutin treatment (Figure 4D). After 2 minutes, we also observed a relatively slower loss of Pol II from the template compared to previous experiments where transcription was inhibited by other means[76]. Additionally, this decrease in Pol II occupancy at later time points does not appear polar as it would if elongation were proceeding normally. These results suggest that thiolutin may have additional non-immediate inhibitory effects on Pol II elongation in vivo (Figure 4D). Together, we conclude that thiolutin can inhibit Pol II initiation both in vitro and in vivo.

To investigate the nature of the inhibitory species, we further examined thiolutin interaction with Mn^{2+}. Interestingly, we observed continuous and reproducible changes of the UV spectra after Mn^{2+} was added to reduced thiolutin (Figure 5A), suggesting changing chemical species in the reaction. The peak of UV absorbance was shifted from 340nm (reduced thiolutin) to around 380nm in the first two minutes, with subsequent decrease in the 380nm peak as a third species at 300nm started to accumulate (Figure 5A). The reaction reached a relative stable equilibrium after 20 minutes. Our data revealed the dynamic change and two major species after Mn^{2+} addition to the reduced thiolutin but could not distinguish how either of these related to the inhibitory species. To test this question, we prepared Thio/Mn^{2+} and either freshly treated Pol II or incubated at room temperature for 20 minutes before treating Pol II (Figure 5B). Remarkably, we observed strong Pol II inhibition by freshly prepared Thio/Mn^{2+} but complete loss of Thio/Mn^{2+} inhibitory activity after 20 minutes (Figure 5B). This result is consistent with the 380nm species possibly contributing to Pol II inhibition yet being unstable in solution. In contrast to the window for inhibitory activity of Thio/Mn^{2+}, immediately treated Pol II was inhibited for up to 50 minutes (20-minute incubation and 30-minute reaction time), suggesting that the Pol II inhibition was stable (Figure 5B).

We propose two models to reconcile the observation that Pol II stabilized the unstable 380nm inhibitory species. First, Pol II might stabilize the inhibitory species in a tight pocket that prevented further reaction into other inactive species. Second, Mn^{2+} might coordinate with reduced thiolutin to form a disulfide bond within Pol II or possibly a thiolutin adduct, as Cu^{2+} does to facilitate disulfide formation through cysteine sulfenylation in other proteins[77-79]. If sulfenylation and disulfide bond formation were involved, the Thio/Mn^{2+} inhibition is expected to be suppressible by a high concentration of DTT. Indeed, we found that excess DTT abolished the inhibition, consistent with the involvement of reductant sensitive inhibition (Figure 5C).

Discussion

Thiolutin is a well-known transcription inhibitor that has been used in mRNA stability studies, but its mode of inhibition has been complicated and unresolved. It has been demonstrated that reduced thiolutin and the related natural product holomycin chelate Zn^{2+} in vitro, and thiolutin chelation of Zn^{2+} could specifically inhibit diverse classes of metalloproteins[10,12]. However, these previous reports tested yet failed to observe direct thiolutin inhibition of RNAPs, under conditions where Zn^{2+} chelation was permissible. Here we present three independent genetic screens for thiolutin resistant or sensitive mutants, providing a genetic basis for understanding thiolutin-altered cellular responses and reveal a direct mode of action against Pol II in vivo. We show that alterations in diverse cellular pathways can modulate cellular sensitivity to thiolutin. In light of our genetic results, we discovered that both reductant DTT and Mn^{2+} together activate thiolutin for direct inhibition of Pol II function, countering the recent narrative while confirming classic observations[10,19].

Thiolutin inhibits Pol II through a novel mode of action

We propose that Thio/Mn^{2+} inhibits Pol II through a novel mode of action. The critical order of treating Pol II with thiolutin prior to template DNA binding is a stereotypical behavior for RNAP clamp inhibitors[22,23,80-83], which are distinct from inhibitors targeting the active site, NTP uptake, or RNA exit channels. In addition, we show that thiolutin inhibits Pol II elongation on an initiation-bypassing transcription bubble template, distinct from all the three characterized *E. coli* RNAP inhibitors that lock the clamp in the closed state (Myx, Cor and Rip) that do not inhibit RNAP elongation[22,84]. It should be noted that Lpm, an inhibitor that appears to lock the clamp in the partially or fully open state[23], has never been tested on a bubble template. Therefore, thiolutin behaves differently from Myx, Cor and Rip, but further experiments are in need to test whether thiolutin behaves similarly to Lpm. Finally, the exact thiolutin binding site on Pol II remains unclear, and our data cannot rule out the possibility that thiolutin may inhibit Pol II regions other than clamp-controlling switch regions.

Diverse cellular pathways modulate thiolutin multiple modes of action

Our genetic screens reveal the contribution of diverse cellular pathways in thiolutin sensitivity. Many of these pathways can be reconciled in a unified model based on current understanding of thiolutin mode of action. In the cell, the thiolutin intra-molecular disulfide bond appears to be reduced, and we propose thioredoxins Trx1 and Trx2 directly or indirectly contribute to thiolutin reduction or are responsive to thiolutin oxidation of other proteins, thereby promoting putative thioredoxin oxidation. Reduced thiolutin subsequently chelates Zn^{2+} to inhibit multiple metalloproteins (*e.g.* Rpn11 and conferring block to proteasomal degradation of substrates), affects Zn^{2+} homeostasis, interacts with Mn^{2+} to inhibit Pol II transcription (and possibly Pol I and III), or become re-oxidized by molecular oxygen. The reduction or redox cycling of thiolutin may induce the observed Yap1 nuclear localization and oxidative stresses. In addition, we have shown that reduced thiolutin may also chelate other divalent metals such as Cu^{2+} (but not Mg^{2+}), but whether other thiolutin-metal complexes have additional activities remain to be further tested.

Thiolutin should be used as a tool with caution

Our work underpins the caveats for using thiolutin to investigate other cellular processes, as suggested by previous studies[9,10,12]. As a routinely used transcription inhibitor to study mRNA stability, it was shown that thiolutin itself inhibits mRNA degradation and complicates the quantitation of mRNA half-life at higher doses[9]. In addition, studies from us and others reveal that thiolutin induces multiple cellular stress through inhibiting various targets, suggesting the lack of thiolutin specificity even at low doses.

Thiolutin mode of action may reveal insights into Pol II pausing

The thiolutin induced pause (and arrest) pattern appears to be highly specific and position-dependent, and it will be interesting to further investigate the pause sequence preference and its possible connection to a specific inhibited Pol II conformation. As discussed above, biochemical properties of thiolutin inhibited Pol II most closely resembles clamp inhibition by a locked non-closed state, possibly a partially or fully open state. It is tempting to hypothesize that the thiolutin-induced pause prone Pol II is linked to a specific Pol II conformation. This hypothesis is also consistent with the observations in E.coli RNAP that paused elongation complexes appear to correlate with open clamp and TL states, which can be reversed and possibly regulated by elongation factor RfaH[85,86]. It has been proposed that this RfaH (a homolog of Spt5 in eukaryotes) pause suppression through the RNAP clamp may be a conserved regulatory mechanism for RNAP elongation in all domains of life[87]. Further

characterization of thiolutin inhibited Pol II may reveal additional insights into this process in eukaryotes.

Material and Methods

Yeast strains and reagents

Yeast strains and primers used are listed in Table S2. *YAP1* C-terminal tagging with EGFP and gene deletion strains were constructed as described[88,89]. Chemicals were commercially obtained from the following: Cayman Chemical (Thiolutin), Gold Biotechnology (DTT, TCEP, 5FOA), Sigma ($MnCl_2$), JT Baker($ZnCl_2$), BDH Chemicals ($MgCl_2$).

Variomics screens

Two separate pools of diploid Variomics libraries were gifts from Dr. Xuewen Pan: one for non-essential and the other for essential genes[28]. The pooled diploid Variomics libraries were grown, sporulated and selected for haploid Variomics libraries as described[28]. Haploid Variomics libraries were subsequently used for the genetic screens. To convert the Variomics libraries into plasmid-free deletion libraries, pooled Variomics libraries (diploid for essential genes and haploid for non-essential genes) were grown in liquid SC media and plated on SC+5FOA plates to select against the mutants with the *URA3* plasmids containing the Variomics mutations. The diversity of the libraries were confirmed by deep sequencing of barcodes ("uptags" and "downtags") flanking the deletion cassettes.

For manual screening of variomics libraries, about 1-3×10^7 cells were plated on SC+10μg/mL thiolutin plates, and the potential thiolutin resistant candidates were restruck out on SC+10μg/mL thiolutin plates to validate the resistance. The plasmids from the validated resistant candidates were subsequently recovered for Sanger sequencing to identify putative resistance-conferring variants. We subsequently tested dominance for the repeatedly isolated candidates. The recovered plasmids from all reproducibly isolated candidates were transformed into the wild-type (CKY457) strain, and thiolutin sensitivity for transformants was phenotyped and compared to the empty vector control.

For high-throughput screens, Variomics libraries were screened on plates, while deletion libraries were screened in liquid, as previously described[24,25,28], and three independent screens (biological replicates) were performed. For Variomics screens, each library was screened on SC-URA+DMSO, SC-URA+8μg/mL thiolutin or SC-URA+10μg/mL plates. Each biological replicate was screened on 9 plates (6×10^7 cells/plate) for 3 days, and cells were scraped to screen for an additional set of 9 plates for 3 days (6×10^7 cells/plate). Deletion libraries were grown in liquid SC media to 3×10^7 cells/mL and diluted in SC+3μg/mL thiolutin (for haploid non-essential gene deletion library) or SC+4μg/mL thiolutin (for diploid essential gene deletion library) to grow for 20 generations. During the selection, the cells were diluted to 1×10^6 cells/mL every five generations to maintain cultures in log phase. For both screens, yeast cells were pooled, and genomic DNA was prepared using a YeaStar Genomic DNA kit (Zymo Research) for subsequent PCR amplification of barcode regions. Amplicons were sequenced by illumina Hiseq2500 in rapid mode. The sequencing reads are deposited in the SRA under the Bioproject PRJNA725683.

Bar-seq data processing

Sequencing reads are mapped to the re-annotated barcode sequences[24] using Bowtie2 (version 2.2.4) with the -N flag set to 0 and the --no-unal flag to suppress unaligned reads for further analyses. Bowtie2 outputs were written into SAM format and further extracted using Samtools (version 1.3.1). Barcode sequences shorter than 15nts or were mapped to multiple reference barcodes were discarded. On average, 98% of sequencing reads were uniquely mapped.

As with Robinson et al.[30], we filtered out barcodes with lower than 100 total reads across all samples, since low count barcodes across all conditions were likely from sequencing errors and did not exist. In addition, mutants with less than 20 reads in both treated and the corresponding untreated controls are further filtered out, to exclude large changes from a small amount of reads with low confidence.

Following Robinson et al.[30], we added 1 pseudo-count to each barcode count to avoid division by 0, and performed TMM normalization using the edgeR package (version 3.12.1). For differential abundance analyses, we used the edgeR to compute mutant specific dispersions, p-value and log transformed abundance changes using exactTest function (default setting). The transformed data were subsequently subjected to differential abundance analyses and clustering analyses. Differential abundance analyses were performed independently for the uptag and downtag sequences, and reproducibility between uptag and downtag data was assessed with Pearson correlation in R. Hierarchical clustering of the thiolutin phenotypic profile to an existing drug response profile for yeast mutants, consisting of 3356 compounds[25] was performed in Cluster (3.0)[90], using centered correlation and complete linkage.

Mutants with significantly altered abundance ($p<0.01$) were subjected to gene-ontology (GO) analyses as previously reported[25]. In brief, all three GO terms, including biological processes (BP), Molecular Function (MF) and Cellular components (CC), were included in our analyses. Following the previous report[25], BP and MF GO terms that are too specific (present in less than 5 genes) or too generic (present in greater than 300 genes) were excluded, although smaller GO term groups were allowed for protein complexes (more than 2 genes) and larger groups (greater than 300 genes) were allowed for cellular components. We computed the GO term enrichment analyses for the significantly resistant or sensitive mutants ($p<0.01$) using hypergeometric test in R (version 3.2.2, physer function, default setting). Raw counts and p-value for each GO term were reported.

A series of quality controls were performed on the reproducibility among biological replicates, consistency between the two barcodes on each gene deletion (uptag and downtag) for the same strain, common and distinct properties between Variomics and Deletion libraries following a well-established statistical analysis pipeline . A subset of the statistically significant resistant or sensitive mutants were further validated by re-constructing the deletion strain for individual phenotyping.

Visualization of Yap1 localization under fluorescence microscopy

Microscopy experiments were performed as previously described[76]. In brief, CKY2038 was grown to mid-log (1-2×10^7 cells/mL) in SC liquid media and added to the ConA treated perfusion chamber gasket (ThermoFisher, 4 chamber: 19 × 6mm) for treatment at indicated conditions (SC+1% DMSO, SC+10μg/mL Thiolutin, SC+10μg/mL Holomycin or SC+0.4mM H_2O_2) under the fluorescence microscope. The procedure to prepare the chamber and the microscope setting were the same as previously described.

Glutathione quantitation assays

WT yeast (CKY457) cultures were grown (in YPD at 30˚C) until mid-log phase (~2×10^7 cells/mL), washed and resuspended in the indicated conditions (YPD+1% DMSO, YPD+10μg/mL Thiolutin or YPD+10μg/mL Holomycin). The suspended culture were grown at 30˚C for one hour, and 5×10^7/mL cells were subject to glutathione (GSH) quantitation. The active and total GSH levels were quantified using the GSH detection kit from Arbor Assays

(K006-F5) following the manual. The glutathione disulfide (GSSG) level was calculated by (Total GSH - Active GSH)/2.

UV-Vis assays

Thiolutin reduction and Zn^{2+} chelation reactions were performed in 250µL reaction with 50µM Thiolutin, 50µM $ZnCl_2$ and 100mM potassium phosphate buffer (pH=6.5), as previously described[1]. Mn^{2+} chelation reaction and relevant controls were performed under almost identical conditions except for the 100mM Tris buffer (pH=8) to keep consistent pH with the *in vitro* transcription assays. Each reaction had 250µL final volume and was quantified in Nanodrop 2000c spectrophotometer using UV-transparent cuvettes.

Growth, viability and canavanine resistance assays

Phenotyping of mutants using plate assays were performed as previously described, with indicated addition of chemicals[91,92]. Yeast liquid growth curve assays with Tecan Infinite F200 plate readers were performed as previously described[76]. For viability assays and canavanine resistance assays, WT yeast strain CKY457 was grown in YPD until mid-log (1-2×10^7 cells/mL), washed and treated with the indicated conditions (YPD, YPD+3µg/mL thiolutin, YPD+5µg/mL thiolutin and YPD+10µg/mL thiolutin) for an hour. The viability was quantified by staining the yeast cells in 0.1% Trypan blue staining (GE Healthcare Life Sciences, Catalog Number SV30084.01) for 3 mins, and the viability was quantified by counting the fraction of unstained yeast cells under the microscope. At least 300 yeast cells were counted in each repeat. Canavanine resistance frequency was quantified by plating the culture onto YPD and SC-Arg+60µg/mL canavanine plates and dividing the number of canavanine resistant colonies by the number of viable colonies on YPD plates. Three experimental replicates were performed.

Pol II transcription activity assays

Pol II was purified using a strain expressing Rpb3 tagged with tandem-affinity tag (TAP), following a procedure as previously described[93]. For initiation experiments DTT was removed from the Pol II buffer prior to the assay using Zeba spin desalting column (Thermo Scientific), though in later experiments this was found to be unnecessary.

Standard ssDNA transcription assays were performed in the *in vitro* transcription buffer (20mM Tris-HCl pH8, 40mM KCl, 5mM $MgCl_2$). Each reaction had ~0.5 pmol Pol II, 2µg denatured sheared salmon sperm DNA as the template and 200µM NTPs except 9µM cold NTP for labeling with that species (UTP or CTP), 1µM radioactive α-^{32}P UTP or CTP (800 Ci/mmol, Perkin-Elmer) as substrates. The concentration of thiolutin, reductants (DTT or TCEP) and $MnCl_2$ varies among the experiments (indicated in each figure). In general, 5 µl pre-treatment reactions including DMSO or thiolutin (at 2X final treatment concentration, from 7.5 µg/mL to 60 µg/mL in DMSO), +/- $MnCl_2$ at specified concentration, and DTT (1-2X molar equivalent to thiolutin) were composed and incubated for 5 minutes at room temperature. To these reactions Pol II was added (with or without pre-binding to DNA) in an equal volume of 2X transcription buffer, yielding 10 µl reactions in 1X transcription buffer for thiolutin treatment. These reactions were incubated for 20 minutes at room temperature. Transcription was initiated by addition of 5 µl DNA/NTP (or just NTP mix in case of pretreatment) and incubated at room temperature for 30 minutes then stopped with stop buffer (10M Urea, 5mM EDTA in TBE). DTT reversal of thiolutin inhibition was accomplished by adding 2 µl 60 mM DTT to 8 µl Pol II treatment reaction at the end of the 20 minute treatment, prior to addition of NTPs/DNA. Transcripts were separated from unincorporated α-^{32}P NTPs on 10% acrylamide/7M urea/TBE gels and visualized with a Bio-Rad Pharos Phosphorimager or GE Typhoon Imager. In vitro transcription elongation assays were performed as previously described[93], with modifications of time in the figure. 5µl reactions comprising 5 pmol Pol II, 40 µg/mL thiolutin in DMSO or DMSO alone, 875 µM MnCl2,

equimolar DTT to thiolutin, 1X transcription buffer, and 3.75 µg BSA were incubated for 20 minutes at room temperature and incubated with 2.5 µl annealed transcription scaffold as described. After 5 minutes, non-template strand was added for an additional 5 minute incubation. Thiolutin-treated Pol II+scaffold was then diluted with additional 1X transcription buffer, MnCl2, thiolutin, while untreated Pol II+scaffold was diluted with thiolutin containing buffer (made fresh) or control buffer with DMSO. After 20 additional minutes at room temperature, reactions proceeded exactly as described in[93].

Yeast strain (CKY1132) containing a C-terminal epitope tag on the Rpb3 (*RPB3::3XFLAG::kanMX4*) subunit of Pol II was used for chromatin immunoprecipitation (ChIP). For in vivo elongation assays, Pol II occupancy over a constitutive promoter-driven reporter (*TEF1p::YLR454w*) was determined after treating the cells with thiolutin. Yeast were grown in SC media to mid-log ($1X10^7$ cells/mL) and treated with 10 µg/mL thiolutin for 2, 4, 8 or 10 mins, cross-linked with 1% formaldehyde solution (1% formaldehyde, 10mM NaCl, 100µM EDTA and 5mM HEPES-KOH, pH 7.5) for 20 minutes and quenched by 3M glycine (final concentration 360mM) for 5 minutes. ChIP and qPCR were performed as described previously[76]. In brief, cross-linked cells were disrupted by bead beating and cell lysate was centrifuged at 1500 rpm for 1 min at 4◦C to remove cell-debris, followed by centrifugation of chromatin pellets, subsequent washing of pellets (twice) with 1 ml FA buffer (50 mM HEPES-KOH pH 7.5, 300 mM NaCl, 1 mM EDTA, 0.1% Triton X-100, 0.01% sodium deoxycholate, 0.1% SDS and 1 mM PMSF) at 14000 rpm for 20 min at 4˚C. Chromatin pellets were sonicated using a Diagenode Bioruptor (45 cycles – 3 × 15 cycles; 30 s ON/45 s OFF) and used for IP with anti-FLAG antibody (FLAG M2 magnetic beads, Sigma-Aldrich). 10% of the total IP material was used as input. Input or immunoprecipitated DNA was purified by standard phenol–chloroform extraction and ethanol precipitated with pellet paint (MilliporeSigma) or glycoblue (ThermoFisher). Immunoprecipitated DNA and 10% of corresponding input DNA (1:10 diluted) were used for qPCR with SsoAdvanced Universal SYBR Green supermix (Bio-Rad) using CFX 96 (Bio-Rad). Pol II fold enrichment was determined by the delta CT method.

1H-NMR characterization of Thiolutin reduction and metal binding

Thiolutin stock solution for NMR experiments was freshly prepared by dissolving thiolutin in DMSO-d6. Thiolutin reduction study was performed using freshly prepared DTT in an NMR tube at the final sample concentrations of 1.5mM thiolutin, 7.5mM DTT, 15mM Tris (pH=8.0) and 10% D2O. 1H-NMR spectra were collected immediately using 500MHz Bruker Avance II spectrometer at 25 ˚C. For Zn^{2+} and Mn^{2+} chelation experiments, Zn^{2+} or Mn^{2+} were added at a final concentration of 7.5mM 1 minute after thiolutin reduction by DTT and were incubated at room temperature for 2 minutes before the acquisition of 1H-NMR spectra.

Acknowledgements

We thank Xuewen Pan for the kind gift of Variomics libraries, and Guillermo Calero for one of the Pol II purifications used here. We acknowledge funding from NIH R01GM097260 to CDK and also Welch Foundation Grant A-1763 to CDK for support on this project while our lab was at Texas A&M University. We acknowledge NSF for funding a Research Experience for Undergraduates site grant DBI-0851611 to Texas A&M Department of Biochemistry and Biophysics for support of AJL, SU, and EMP.

References

1. Li, B. & Walsh, C.T. Streptomyces clavuligerus HlmI is an intramolecular disulfide-forming dithiol oxidase in holomycin biosynthesis. *Biochemistry* **50**, 4615-4622 (2011)
2. Li, B., Wever, W.J., Walsh, C.T. & Bowers, A.A. Dithiolopyrrolones: biosynthesis, synthesis, and activity of a unique class of disulfide-containing antibiotics. *Nat Prod Rep* **31**, 905-23 (2014).PMC4132845
3. Rossini, C., Taylor, W., Fagan, T. & Hastings, J.W. Lifetimes of mRNAs for clock-regulated proteins in a dinoflagellate. *Chronobiol Int* **20**, 963-76 (2003)
4. Grigull, J., Mnaimneh, S., Pootoolal, J., Robinson, M.D. & Hughes, T.R. Genome-wide analysis of mRNA stability using transcription inhibitors and microarrays reveals posttranscriptional control of ribosome biogenesis factors. *Molecular and cellular biology* **24**, 5534-5547 (2004)
5. Kebaara, B.W., Nielsen, L.E., Nickerson, K.W. & Atkin, A.L. Determination of mRNA half-lives in Candida albicans using thiolutin as a transcription inhibitor. *Genome* **49**, 894-899 (2006)
6. Morey, J.S. & Van Dolah, F.M. Global analysis of mRNA half-lives and de novo transcription in a dinoflagellate, Karenia brevis. *PLoS One* **8**, e66347 (2013).PMC3679056
7. Bergmann, R. Thiolutin inhibits utilization of glucose and other carbon sources in cells of Escherichia coli. *Antonie Van Leeuwenhoek* **55**, 143-52 (1989)
8. Monje-Casas, F., MICHáN, C. & Pueyo, C. Absolute transcript levels of thioredoxin-and glutathione-dependent redox systems in Saccharomyces cerevisiae: response to stress and modulation with growth. *Biochemical Journal* **383**, 139-147 (2004)
9. Pelechano, V. & Perez-Ortin, J.E. The transcriptional inhibitor thiolutin blocks mRNA degradation in yeast. *Yeast* **25**, 85-92 (2008)
10. Lauinger, L., Li, J., Shostak, A., Cemel, I.A., Ha, N., Zhang, Y., Merkl, P.E., Obermeyer, S., Stankovic-Valentin, N. & Schafmeier, T. Thiolutin is a zinc chelator that inhibits the Rpn11 and other JAMM metalloproteases. *Nature Chemical Biology* **13**, 709-714 (2017)
11. Eshleman, N., Luo, X., Capaldi, A. & Buchan, J.R. Alterations of signaling pathways in response to chemical perturbations used to measure mRNA decay rates in yeast. *RNA* **26**, 10-18 (2020)
12. Chan, A.N., Shiver, A.L., Wever, W.J., Razvi, S.Z., Traxler, M.F. & Li, B. Role for dithiolopyrrolones in disrupting bacterial metal homeostasis. *Proc Natl Acad Sci U S A* **114**, 2717-2722 (2017).PMC5347557
13. Fuchs, A.C., Maldoner, L., Wojtynek, M., Hartmann, M.D. & Martin, J. Rpn11-mediated ubiquitin processing in an ancestral archaeal ubiquitination system. *Nature communications* **9**, 1-12 (2018)
14. Baell, J.B. Redox-active nuisance screening compounds and their classification. *Drug Discovery Today* **16**, 840-841 (2011)
15. Johnston, P.A. Redox cycling compounds generate H 2 O 2 in HTS buffers containing strong reducing reagents—real hits or promiscuous artifacts? *Current opinion in chemical biology* **15**, 174-182 (2011)
16. Khachatourians, G.G. & Tipper, D.J. In vivo effect of thiolutin on cell growth and macromolecular synthesis in Escherichia coli. *Antimicrob Agents Chemother* **6**, 304-10 (1974).PMC444641
17. Joshi, A., Verma, M. & Chakravorty, M. Thiolutin-resistant mutants of Salmonella typhimurium. *Antimicrob Agents Chemother* **22**, 541-7 (1982).PMC183790
18. Roza, J., Blanco, M.G., Hardisson, C. & Salas, J.A. Self-resistance in actinomycetes producing inhibitors of RNA polymerase. *J Antibiot (Tokyo)* **39**, 609-12 (1986)

19. Tipper, D.J. Inhibition of yeast ribonucleic acid polymerases by thiolutin. *J Bacteriol* **116**, 245-56 (1973).PMC246415
20. Sivasubramanian, N. & Jayaraman, R. Thiolutin resistant mutants of Escherichia coli are they RNA chain initiation mutants? *Molecular and General Genetics MGG* **145**, 89-96 (1976)
21. Oliva, B., O'Neill, A., Wilson, J.M., O'Hanlon, P.J. & Chopra, I. Antimicrobial properties and mode of action of the pyrrothine holomycin. *Antimicrob Agents Chemother* **45**, 532-9 (2001).PMC90323
22. Mukhopadhyay, J., Das, K., Ismail, S., Koppstein, D., Jang, M., Hudson, B., Sarafianos, S., Tuske, S., Patel, J. & Jansen, R. The RNA polymerase “switch region” is a target for inhibitors. *Cell* **135**, 295-307 (2008)
23. Wang, D. *Ensemble fluorescence resonance energy transfer analysis of RNA polymerase clamp conformation*, (Rutgers The State University of New Jersey-New Brunswick, 2008).
24. Smith, A.M., Heisler, L.E., Mellor, J., Kaper, F., Thompson, M.J., Chee, M., Roth, F.P., Giaever, G. & Nislow, C. Quantitative phenotyping via deep barcode sequencing. *Genome Res* **19**, 1836-42 (2009).PMC2765281
25. Lee, A.Y., Onge, R.P.S., Proctor, M.J., Wallace, I.M., Nile, A.H., Spagnuolo, P.A., Jitkova, Y., Gronda, M., Wu, Y. & Kim, M.K. Mapping the Cellular Response to Small Molecules Using Chemogenomic Fitness Signatures. *Science* **344**, 208-211 (2014)
26. Parsons, A.B., Lopez, A., Givoni, I.E., Williams, D.E., Gray, C.A., Porter, J., Chua, G., Sopko, R., Brost, R.L., Ho, C.H., Wang, J., Ketela, T., Brenner, C., Brill, J.A., Fernandez, G.E., Lorenz, T.C., Payne, G.S., Ishihara, S., Ohya, Y., Andrews, B., Hughes, T.R., Frey, B.J., Graham, T.R., Andersen, R.J. & Boone, C. Exploring the mode-of-action of bioactive compounds by chemical-genetic profiling in yeast. *Cell* **126**, 611-25 (2006)
27. Birkeland, S.R., Jin, N., Ozdemir, A.C., Lyons, R.H., Jr., Weisman, L.S. & Wilson, T.E. Discovery of mutations in Saccharomyces cerevisiae by pooled linkage analysis and whole-genome sequencing. *Genetics* **186**, 1127-37 (2010).PMC2998298
28. Huang, Z., Chen, K., Zhang, J., Li, Y., Wang, H., Cui, D., Tang, J., Liu, Y., Shi, X., Li, W., Liu, D., Chen, R., Sucgang, R.S. & Pan, X. A functional variomics tool for discovering drug-resistance genes and drug targets. *Cell Rep* **3**, 577-85 (2013).PMC3594652
29. Karim, A.S., Curran, K.A. & Alper, H.S. Characterization of plasmid burden and copy number in Saccharomyces cerevisiae for optimization of metabolic engineering applications. *FEMS yeast research* **13**, 107-116 (2013)
30. Robinson, D.G., Chen, W., Storey, J.D. & Gresham, D. Design and analysis of Bar-seq experiments. *G3 (Bethesda)* **4**, 11-8 (2014).PMC3887526
31. Kuge, S., Jones, N. & Nomoto, A. Regulation of yAP-1 nuclear localization in response to oxidative stress. *EMBO J* **16**, 1710-20 (1997).PMC1169774
32. Wemmie, J.A., Steggerda, S.M. & Moye-Rowley, W.S. The Saccharomyces cerevisiae AP-1 protein discriminates between oxidative stress elicited by the oxidants H2O2 and diamide. *Journal of Biological Chemistry* **272**, 7908-7914 (1997)
33. Coleman, S.T., Epping, E.A., Steggerda, S.M. & Moye-Rowley, W.S. Yap1p activates gene transcription in an oxidant-specific fashion. *Mol Cell Biol* **19**, 8302-13 (1999).PMC84914
34. Kuge, S., Arita, M., Murayama, A., Maeta, K., Izawa, S., Inoue, Y. & Nomoto, A. Regulation of the yeast Yap1p nuclear export signal is mediated by redox signal-induced reversible disulfide bond formation. *Molecular and cellular biology* **21**, 6139-6150 (2001)
35. Gulshan, K., Rovinsky, S.A., Coleman, S.T. & Moye-Rowley, W.S. Oxidant-specific folding of Yap1p regulates both transcriptional activation and nuclear localization. *Journal of Biological Chemistry* **280**, 40524-40533 (2005)

36. Alarco, A.M., Balan, I., Talibi, D., Mainville, N. & Raymond, M. AP1-mediated multidrug resistance in Saccharomyces cerevisiae requires FLR1 encoding a transporter of the major facilitator superfamily. *J Biol Chem* **272**, 19304-13 (1997)
37. Coleman, S.T., Tseng, E. & Moye-Rowley, W.S. Saccharomyces cerevisiae basic region-leucine zipper protein regulatory networks converge at the ATR1 structural gene. *Journal of Biological Chemistry* **272**, 23224-23230 (1997)
38. Gulshan, K. & Moye-Rowley, W.S. Multidrug resistance in fungi. *Eukaryot Cell* **6**, 1933-42 (2007).PMC2168405
39. Meyer, Y., Buchanan, B.B., Vignols, F. & Reichheld, J.P. Thioredoxins and glutaredoxins: unifying elements in redox biology. *Annu Rev Genet* **43**, 335-67 (2009)
40. Winzeler, E.A., Shoemaker, D.D., Astromoff, A., Liang, H., Anderson, K., Andre, B., Bangham, R., Benito, R., Boeke, J.D., Bussey, H., Chu, A.M., Connelly, C., Davis, K., Dietrich, F., Dow, S.W., El Bakkoury, M., Foury, F., Friend, S.H., Gentalen, E., Giaever, G., Hegemann, J.H., Jones, T., Laub, M., Liao, H., Liebundguth, N., Lockhart, D.J., Lucau-Danila, A., Lussier, M., M'Rabet, N., Menard, P., Mittmann, M., Pai, C., Rebischung, C., Revuelta, J.L., Riles, L., Roberts, C.J., Ross-MacDonald, P., Scherens, B., Snyder, M., Sookhai-Mahadeo, S., Storms, R.K., Veronneau, S., Voet, M., Volckaert, G., Ward, T.R., Wysocki, R., Yen, G.S., Yu, K., Zimmermann, K., Philippsen, P., Johnston, M. & Davis, R.W. Functional characterization of the S. cerevisiae genome by gene deletion and parallel analysis. *Science* **285**, 901-6 (1999)
41. Machado, A.K., Morgan, B.A. & Merrill, G.F. Thioredoxin reductase-dependent inhibition of MCB cell cycle box activity in Saccharomyces cerevisiae. *J Biol Chem* **272**, 17045-54 (1997)
42. Carmel-Harel, O., Stearman, R., Gasch, A.P., Botstein, D., Brown, P.O. & Storz, G. Role of thioredoxin reductase in the Yap1p-dependent response to oxidative stress in Saccharomyces cerevisiae. *Mol Microbiol* **39**, 595-605 (2001)
43. Trotter, E.W. & Grant, C.M. Thioredoxins are required for protection against a reductive stress in the yeast Saccharomyces cerevisiae. *Mol Microbiol* **46**, 869-78 (2002)
44. Hacioglu, E., Esmer, I., Fomenko, D.E., Gladyshev, V.N. & Koc, A. The roles of thiol oxidoreductases in yeast replicative aging. *Mech Ageing Dev* **131**, 692-9 (2010).PMC3311284
45. Ragu, S., Dardalhon, M., Sharma, S., Iraqui, I., Buhagiar-Labarchede, G., Grondin, V., Kienda, G., Vernis, L., Chanet, R., Kolodner, R.D., Huang, M.E. & Faye, G. Loss of the thioredoxin reductase Trr1 suppresses the genomic instability of peroxiredoxin tsa1 mutants. *PLoS One* **9**, e108123 (2014).PMC4172583
46. Grant, C.M., Perrone, G. & Dawes, I.W. Glutathione and Catalase Provide Overlapping Defenses for Protection against Hydrogen Peroxide in the YeastSaccharomyces cerevisiae. *Biochemical and biophysical research communications* **253**, 893-898 (1998)
47. Castro, F.A., Mariani, D., Panek, A.D., Eleutherio, E.C. & Pereira, M.D. Cytotoxicity mechanism of two naphthoquinones (menadione and plumbagin) in Saccharomyces cerevisiae. *PLoS One* **3**, e3999 (2008).PMC2600608
48. Toledano, M.B., Delaunay-Moisan, A., Outten, C.E. & Igbaria, A. Functions and cellular compartmentation of the thioredoxin and glutathione pathways in yeast. *Antioxid Redox Signal* **18**, 1699-711 (2013).PMC3771550
49. Jung, U., Zheng, X., Yoon, S.O. & Chung, A.S. Se-methylselenocysteine induces apoptosis mediated by reactive oxygen species in HL-60 cells. *Free Radic Biol Med* **31**, 479-89 (2001)
50. Ravi, D. & Das, K.C. Redox-cycling of anthracyclines by thioredoxin system: increased superoxide generation and DNA damage. *Cancer Chemother Pharmacol* **54**, 449-58 (2004)

51. Jimenez, A., Tipper, D.J. & Davies, J. Mode of action of thiolutin, an inhibitor of macromolecular synthesis in Saccharomyces cerevisiae. *Antimicrob Agents Chemother* **3**, 729-38 (1973).PMC444489
52. Dudley, A.M., Janse, D.M., Tanay, A., Shamir, R. & Church, G.M. A global view of pleiotropy and phenotypically derived gene function in yeast. *Mol Syst Biol* **1**, 2005 0001 (2005).PMC1681449
53. Pagani, M.A., Casamayor, A., Serrano, R., Atrian, S. & Arino, J. Disruption of iron homeostasis in Saccharomyces cerevisiae by high zinc levels: a genome-wide study. *Mol Microbiol* **65**, 521-37 (2007)
54. Ruotolo, R., Marchini, G. & Ottonello, S. Membrane transporters and protein traffic networks differentially affecting metal tolerance: a genomic phenotyping study in yeast. *Genome Biol* **9**, R67 (2008).PMC2643938
55. Bleackley, M.R., Young, B.P., Loewen, C.J. & MacGillivray, R.T. High density array screening to identify the genetic requirements for transition metal tolerance in Saccharomyces cerevisiae. *Metallomics* **3**, 195-205 (2011)
56. Jiang, L., Cao, C., Zhang, L., Lin, W., Xia, J., Xu, H. & Zhang, Y. Cadmium-induced activation of high osmolarity glycerol pathway through its Sln1 branch is dependent on the MAP kinase kinase kinase Ssk2, but not its paralog Ssk22, in budding yeast. *FEMS Yeast Res* **14**, 1263-72 (2014)
57. Acosta-Alvear, D., Cho, M.Y., Wild, T., Buchholz, T.J., Lerner, A.G., Simakova, O., Hahn, J., Korde, N., Landgren, O., Maric, I., Choudhary, C., Walter, P., Weissman, J.S. & Kampmann, M. Paradoxical resistance of multiple myeloma to proteasome inhibitors by decreased levels of 19S proteasomal subunits. *Elife* **4**, e08153 (2015).PMC4602331
58. Tsvetkov, P., Mendillo, M.L., Zhao, J., Carette, J.E., Merrill, P.H., Cikes, D., Varadarajan, M., van Diemen, F.R., Penninger, J.M. & Goldberg, A.L. Compromising the 19S proteasome complex protects cells from reduced flux through the proteasome. *Elife* **4**, e08467 (2015)
59. Tsvetkov, P., Sokol, E., Jin, D., Brune, Z., Thiru, P., Ghandi, M., Garraway, L.A., Gupta, P.B., Santagata, S., Whitesell, L. & Lindquist, S. Suppression of 19S proteasome subunits marks emergence of an altered cell state in diverse cancers. *Proc Natl Acad Sci U S A* **114**, 382-387 (2017).PMC5240730
60. Bandara, P.D., Flattery-O'Brien, J.A., Grant, C.M. & Dawes, I.W. Involvement of the Saccharomyces cerevisiae UTH1 gene in the oxidative-stress response. *Curr Genet* **34**, 259-68 (1998)
61. Wu, C.-Y., Bird, A.J., Winge, D.R. & Eide, D.J. Regulation of the yeast TSA1 peroxiredoxin by ZAP1 is an adaptive response to the oxidative stress of zinc deficiency. *Journal of Biological Chemistry* **282**, 2184-2195 (2007)
62. Wu, C.-Y., Roje, S., Sandoval, F.J., Bird, A.J., Winge, D.R. & Eide, D.J. Repression of sulfate assimilation is an adaptive response of yeast to the oxidative stress of zinc deficiency. *Journal of Biological Chemistry* **284**, 27544-27556 (2009)
63. Wu, C.-Y., Steffen, J. & Eide, D.J. Cytosolic superoxide dismutase (SOD1) is critical for tolerating the oxidative stress of zinc deficiency in yeast. *PloS one* **4**, e7061 (2009)
64. Rudolph, H.K., Antebi, A., Fink, G.R., Buckley, C.M., Dorman, T.E., LeVitre, J., Davidow, L.S., Mao, J.I. & Moir, D.T. The yeast secretory pathway is perturbed by mutations in PMR1, a member of a Ca2+ ATPase family. *Cell* **58**, 133-45 (1989)
65. Mandal, D., Woolf, T.B. & Rao, R. Manganese selectivity of pmr1, the yeast secretory pathway ion pump, is defined by residue gln783 in transmembrane segment 6. Residue Asp778 is essential for cation transport. *J Biol Chem* **275**, 23933-8 (2000)
66. D'Aurora, V., Stern, A.M. & Sigman, D.S. 1,10-Phenanthroline-cuprous ion complex, a potent inhibitor of DNA and RNA polymerases. *Biochem Biophys Res Commun* **80**, 1025-32 (1978)

67. Perrin, D.M., Pearson, L., Mazumder, A. & Sigman, D.S. Inhibition of prokaryotic and eukaryotic transcription by the 2:1 2,9-dimethyl-1,10-phenanthroline-cuprous complex, a ligand specific for open complexes. *Gene* **149**, 173-8 (1994)
68. Reimann, C.W., Block, S. & Perloff, A. The Crystal and Molecular Structure of Dichloro (1, 10-phenanthroline) zinc. *Inorganic Chemistry* **5**, 1185-1189 (1966)
69. Niyogi, S.K., Feldman, R.P. & Hoffman, D.J. Selective effects of metal ions on RNA synthesis rates. *Toxicology* **22**, 9-21 (1981)
70. Lin, S.-J. & Culotta, V.C. Suppression of oxidative damage by Saccharomyces cerevisiae ATX2, which encodes a manganese-trafficking protein that localizes to Golgi-like vesicles. *Molecular and Cellular Biology* **16**, 6303-6312 (1996)
71. Portnoy, M.E., Liu, X.F. & Culotta, V.C. Saccharomyces cerevisiae expresses three functionally distinct homologues of the nramp family of metal transporters. *Mol Cell Biol* **20**, 7893-902 (2000).PMC86400
72. Jensen, L.T., Ajua-Alemanji, M. & Culotta, V.C. The Saccharomyces cerevisiae high affinity phosphate transporter encoded by PHO84 also functions in manganese homeostasis. *Journal of Biological Chemistry* **278**, 42036-42040 (2003)
73. Mei, Y., Jensen, L.T., Gardner, A.J. & Culotta, V.C. Manganese toxicity and Saccharomyces cerevisiae Mam3p, a member of the ACDP (ancient conserved domain protein) family. *Biochemical Journal* **386**, 479-487 (2005)
74. Reddi, A.R., Jensen, L.T., Naranuntarat, A., Rosenfeld, L., Leung, E., Shah, R. & Culotta, V.C. The overlapping roles of manganese and Cu/Zn SOD in oxidative stress protection. *Free Radic Biol Med* **46**, 154-62 (2009).PMC2707084
75. Walmacq, C., Kireeva, M.L., Irvin, J., Nedialkov, Y., Lubkowska, L., Malagon, F., Strathern, J.N. & Kashlev, M. Rpb9 subunit controls transcription fidelity by delaying NTP sequestration in RNA polymerase II. *J Biol Chem* **284**, 19601-12 (2009).PMC2740586
76. Malik, I., Qiu, C., Snavely, T. & Kaplan, C.D. Wide-ranging and unexpected consequences of altered Pol II catalytic activity in vivo. *Nucleic Acids Res* **45**, 4431-4451 (2017).PMC5416818
77. Pecci, L., Montefoschi, G., Musci, G. & Cavallini, D. Novel findings on the copper catalysed oxidation of cysteine. *Amino Acids* **13**, 355-367 (1997)
78. Prudent, M. & Girault, H.H. The role of copper in cysteine oxidation: study of intra- and inter-molecular reactions in mass spectrometry. *Metallomics* **1**, 157-65 (2009)
79. Fetherolf, M.M., Boyd, S.D., Taylor, A.B., Kim, H.J., Wohlschlegel, J.A., Blackburn, N.J., Hart, P.J., Winge, D.R. & Winkler, D.D. Copper-zinc superoxide dismutase is activated through a sulfenic acid intermediate at a copper ion entry site. *Journal of Biological Chemistry* **292**, 12025-12040 (2017)
80. Sergio, S., Pirali, G., White, R. & Parenti, F. Lipiarmycin, a new antibiotic from Actinoplanes III. Mechanism of action. *J Antibiot (Tokyo)* **28**, 543-9 (1975)
81. Talpaert, M., Campagnari, F. & Clerici, L. Lipiarmycin: an antibiotic inhibiting nucleic acid polymerases. *Biochem Biophys Res Commun* **63**, 328-34 (1975)
82. Sonenshein, A.L. & Alexander, H.B. Initiation of transcription in vitro is inhibited by lipiarmycin. *Journal of molecular biology* **127**, 55-72 (1979)
83. Srivastava, A., Talaue, M., Liu, S., Degen, D., Ebright, R.Y., Sineva, E., Chakraborty, A., Druzhinin, S.Y., Chatterjee, S. & Mukhopadhyay, J. New target for inhibition of bacterial RNA polymerase:'switch region'. *Current opinion in microbiology* **14**, 532-543 (2011)
84. Chakraborty, A., Wang, D., Ebright, Y.W., Korlann, Y., Kortkhonjia, E., Kim, T., Chowdhury, S., Wigneshweraraj, S., Irschik, H., Jansen, R., Nixon, B.T., Knight, J., Weiss, S. & Ebright, R.H. Opening and closing of the bacterial RNA polymerase clamp. *Science* **337**, 591-5 (2012).PMC3626110

85. Nayak, D., Voss, M., Windgassen, T., Mooney, R.A. & Landick, R. Cys-pair reporters detect a constrained trigger loop in a paused RNA polymerase. *Mol Cell* **50**, 882-93 (2013).PMC4037917
86. Hein, P.P., Kolb, K.E., Windgassen, T., Bellecourt, M.J., Darst, S.A., Mooney, R.A. & Landick, R. RNA polymerase pausing and nascent-RNA structure formation are linked through clamp-domain movement. *Nat Struct Mol Biol* **21**, 794-802 (2014).PMC4156911
87. Werner, F. A nexus for gene expression-molecular mechanisms of Spt5 and NusG in the three domains of life. *J Mol Biol* **417**, 13-27 (2012).PMC3382729
88. Janke, C., Magiera, M.M., Rathfelder, N., Taxis, C., Reber, S., Maekawa, H., Moreno-Borchart, A., Doenges, G., Schwob, E., Schiebel, E. & Knop, M. A versatile toolbox for PCR-based tagging of yeast genes: new fluorescent proteins, more markers and promoter substitution cassettes. *Yeast* **21**, 947-62 (2004)
89. Chee, M.K. & Haase, S.B. New and redesigned pRS plasmid shuttle vectors for genetic manipulation of Saccharomyces cerevisiae. *G3: Genes, Genomes, Genetics* **2**, 515-526 (2012)
90. De Hoon, M.J., Imoto, S., Nolan, J. & Miyano, S. Open source clustering software. *Bioinformatics* **20**, 1453-1454 (2004)
91. Kaplan, C.D., Jin, H., Zhang, I.L. & Belyanin, A. Dissection of Pol II trigger loop function and Pol II activity-dependent control of start site selection in vivo. *PLoS Genet* **8**, e1002627 (2012).PMC3325174
92. Qiu, C., Erinne, O.C., Dave, J.M., Cui, P., Jin, H., Muthukrishnan, N., Tang, L.K., Babu, S.G., Lam, K.C., Vandeventer, P.J., Strohner, R., Van den Brulle, J., Sze, S.H. & Kaplan, C.D. High-Resolution Phenotypic Landscape of the RNA Polymerase II Trigger Loop. *PLoS Genet* **12**, e1006321 (2016).PMC5127505 the Slonomics DNA synthesis technology utilized in the manuscript.
93. Kaplan, C.D., Larsson, K.M. & Kornberg, R.D. The RNA polymerase II trigger loop functions in substrate selection and is directly targeted by alpha-amanitin. *Mol Cell* **30**, 547-56 (2008).PMC2475549

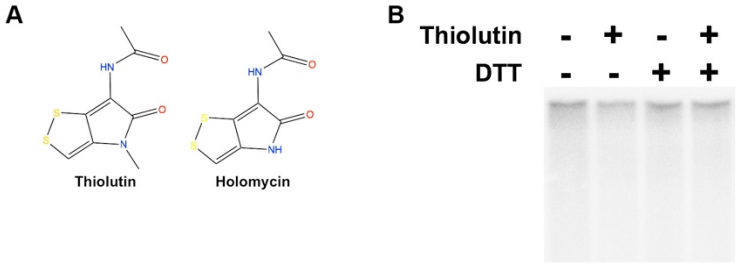

Figure 1. Thiolutin or reduced thiolutin alone fails to inhibit purified yeast Pol II *in vitro*.
(A) Thiolutin and holomycin structures
(B) Thiolutin, or thiolutin treated with equimolar DTT, show no inhibition of Pol II transcription *in vitro*. Transcription activity assay was performed with ssDNA as the template and NTPs, including ^{32}P labeled UTP. The transcribed ^{32}P containing RNA was separated from free ^{32}P UTPs on 10% polyacrylamide gels for visualization. Experiments were performed with at least three times, and a representative experiment is shown.

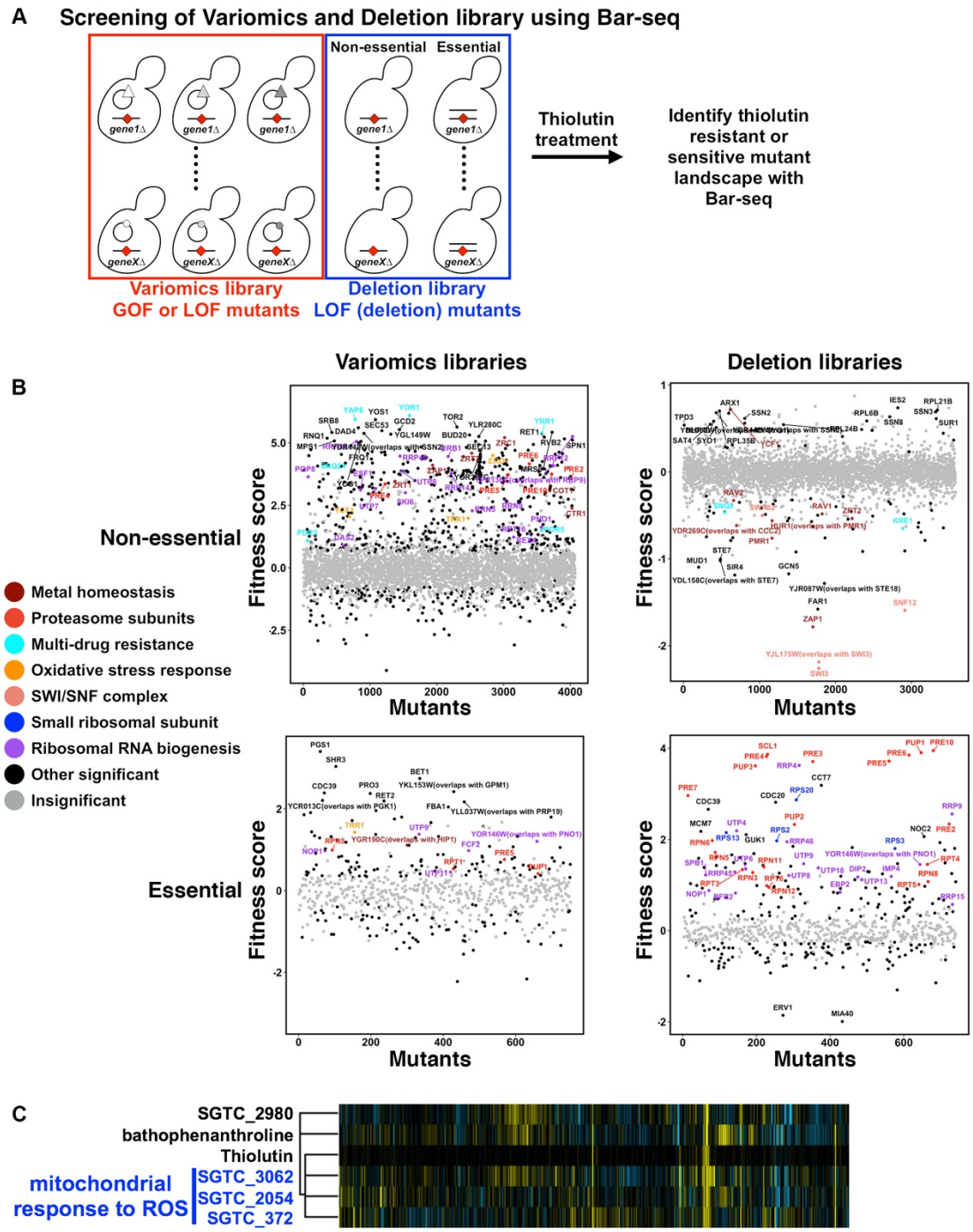

Figure 2. Mutations in diverse cellular pathways confer resistance/sensitivity to thiolutin. (A) Four libraries (Variomics libraries for non-essential or essential genes, Deletion libraries for non-essential or essential genes) were used for screening thiolutin resistant or sensitive

mutants. Changes in abundance in the library was detected by deep sequencing of the PCR amplicon of the barcode region (Bar-seq). Variomics libraries consist of random gene variants and can be used to screen for both Gain-of-Function (GOF) and Loss-of-Function (LOF) alleles, whereas “Deletion” libraries consist of single-gene-deleted mutants that can be used to screen for complete LOF mutants.
(B) Different thiolutin resistant or sensitive mutant classes are revealed in the Bar-seq based screenings of pooled Variomics and Deletion libraries.
(C) Thiolutin induced phenotypic profile in the pooled deletion libraries co-clusters with drugs with signature of “mitochondrial response to ROS”[25] and bathophenanthroline, a metal chelator. 4683 deletion mutants’ responses (in columns) to 3356 compounds (in rows) were used for hierarchical clustering, but only the thiolutin closely correlated compounds are shown in this figure for clarity. Resistant strains: yellow; Sensitive strains: blue.

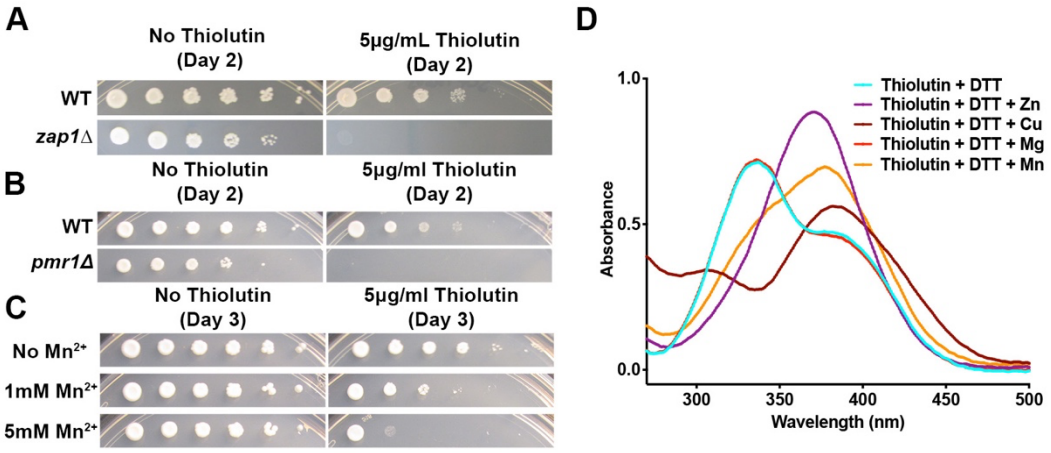

Figure 3. Divalent metals cations appear to alter thiolutin sensitivity *in vivo* and interact with reduced thiolutin *in vitro*. (A-C) 10-fold serial dilutions of yeast strains spotted onto different types of media to examine thiolutin sensitivity. (A) *zap1*Δ is hypersensitive to thiolutin. (B) *pmr1*Δ is hypersensitive to thiolutin. (C) Mn^{2+} supplementation exacerbates WT yeast sensitivity to thiolutin. (D) Reduced thiolutin was incubated with a selection of divalent metal cations and UV absorbance was analyzed. Zn^{2+} , Mn^{2+}, and Cu^{2+}, but not Mg^{2+}, interact with reduced thiolutin, as evident by alteration of the UV spectra of reduced thiolutin.

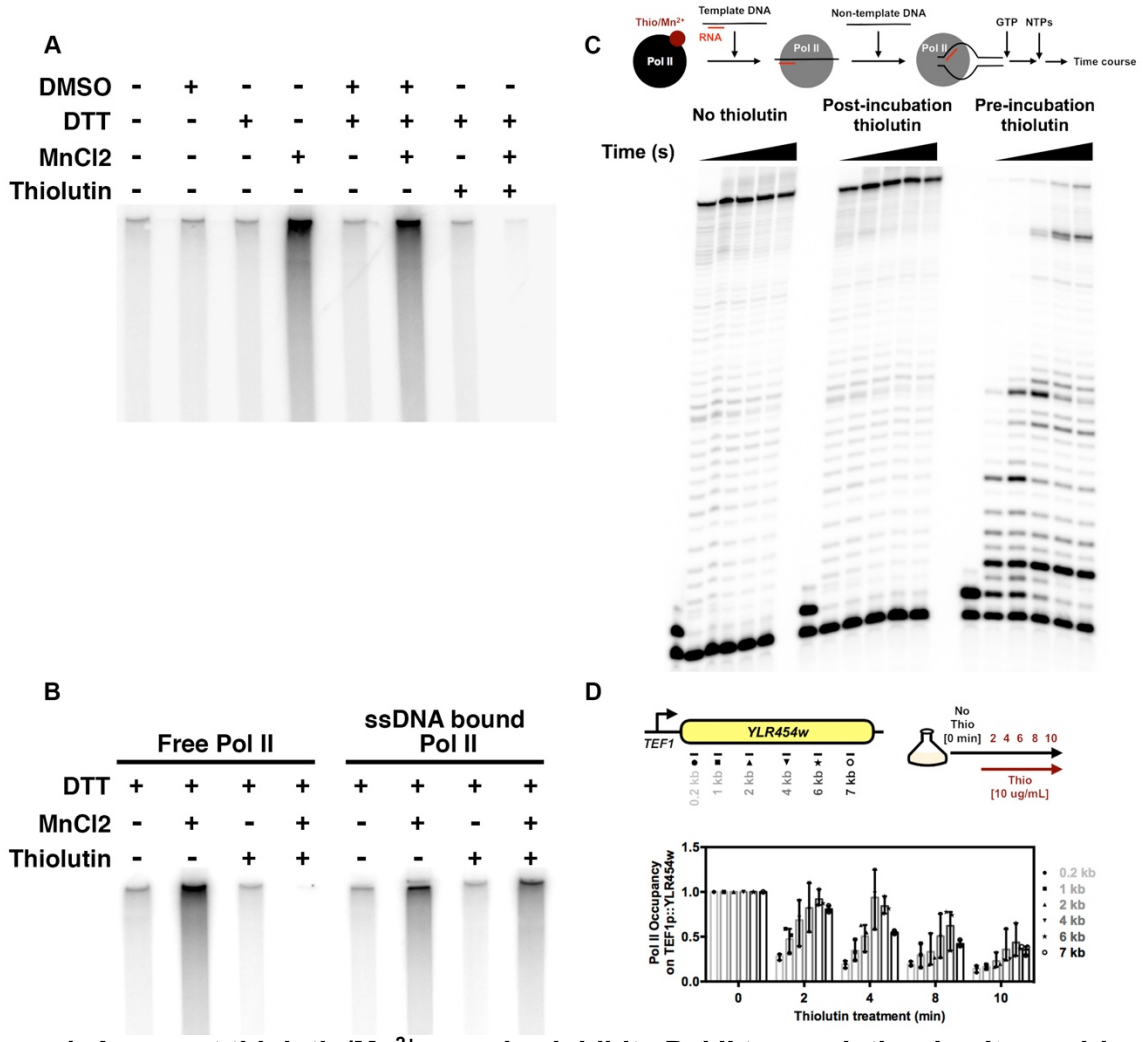

Figure 4. Apparent thiolutin/Mn^{2+} complex inhibits Pol II transcription *in vitro* and *in vivo*. (A) Thiolutin requires both DTT (reductant) and Mn^{2+} to inhibit Pol II transcription *in vitro*. A representative of multiple experiments is shown. Quantifications of this and a wide range of experimental conditions for thiolutin inhibition are shown in Figure S10. (B) Pre-binding to DNA renders Pol II resistant to Thiolutin/Mn^{2+} complex. This gel is representative of multiple independent experiments (Quantifications shown in Figure S10). (C) Thio/Mn^{2+} inhibited Pol II can be manually assembled into a distinct and slow elongating complex. Two experimental replicates were performed, and a representative replicate is shown. (D) Thio/DTT/Mn^{2+} inhibits Pol II transcription *in vivo.* Three experimental replicates were performed, and the error bars represent standard deviation of the mean.

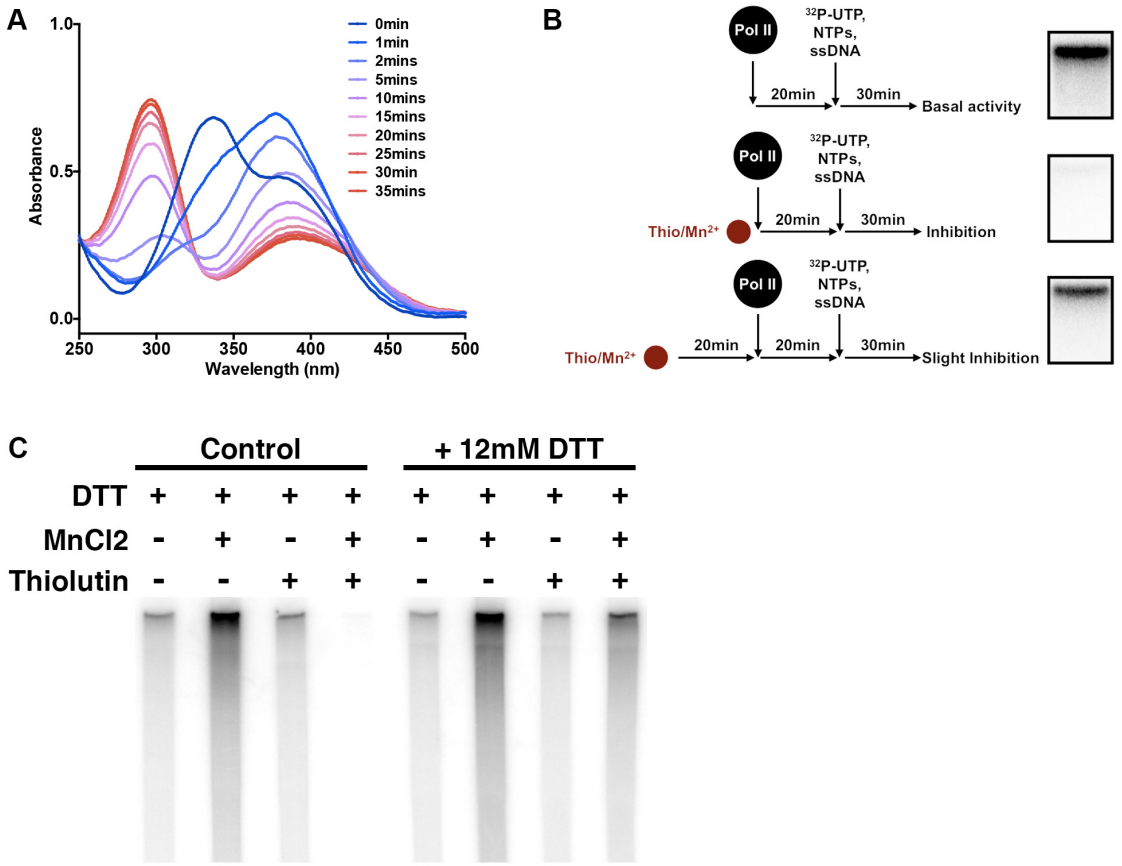

Figure 5. The apparent Thiolutin/Mn^{2+} complex is unstable in solution but stable in Pol II. (A) Time course of changing UV spectra of reduced thiolutin treated with Mn^{2+}. Reduced thiolutin (blue, 0 min) was treated with equivalent molar Mn^{2+}, and the UV spectra was acquired at different time points. Spectra over time was colored in a series of gradient from blue to red. Three experimental replicates were performed, and a representative replicate is shown. (B) Thio/Mn^{2+} lost inhibitory activity after 20 mins in solution though immediately treated Pol II remains inhibited. Two experimental replicates were performed and consistent. One replicate is shown. (C) Thio/Mn^{2+} can be reversed by excess DTT. Excess of DTT was added after 20 minutes of Pol II inhibition by Thio/Mn^{2+}. DTT was at 12 mM during thiolutin treatment. Two replicates under these exact conditions were performed, and a representative replicate is shown. Quantification is shown in Figure S10. Results are representative of additional experiments performed under slightly different conditions.

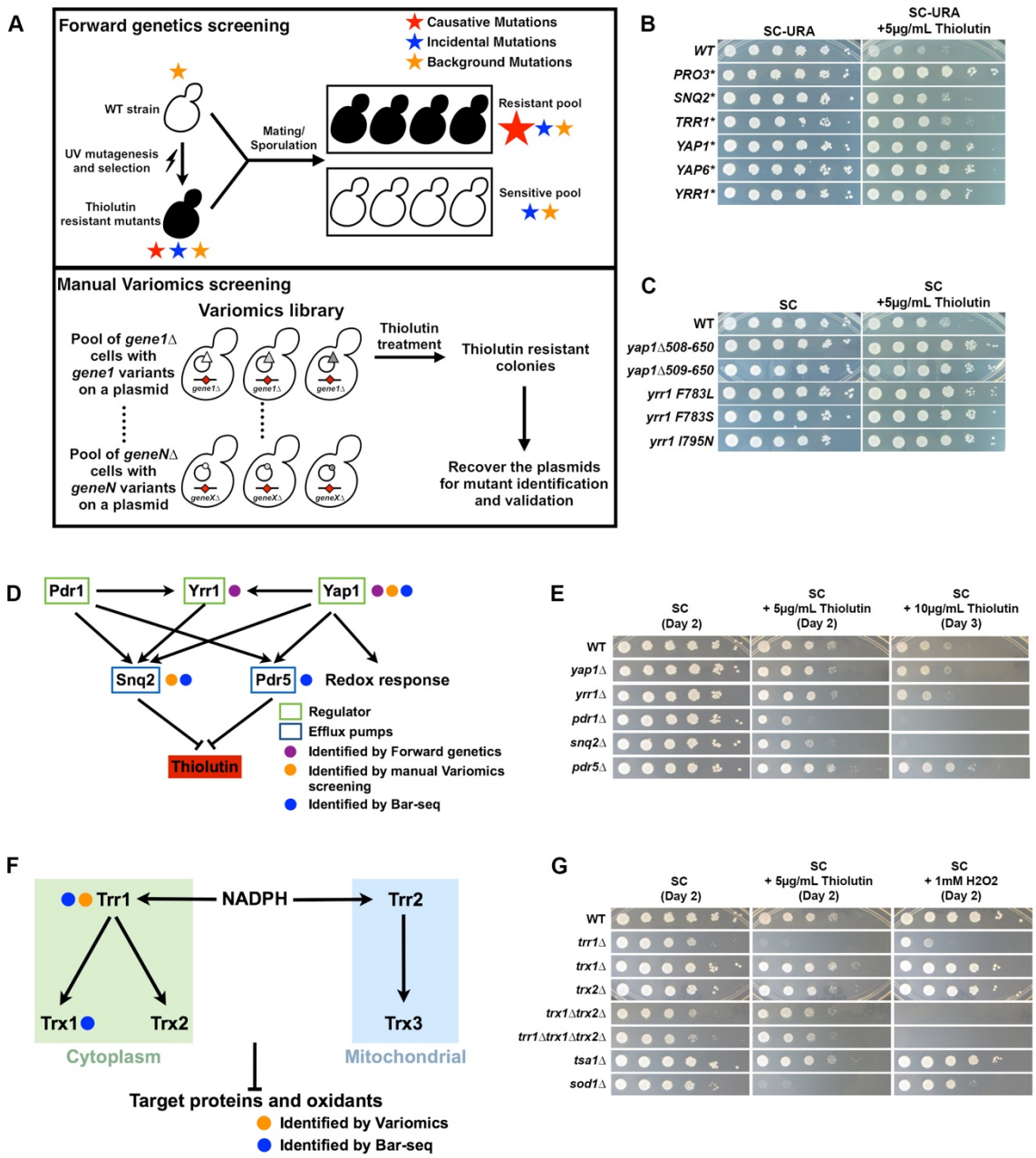

Figure S1. Mutations in multiple drug resistance (MDR) and oxidative stress responses (OSR) pathways alters cellular sensitivity to thiolutin.
(A) Schematic diagram of the two independent genetic screens for thiolutin resistant mutants. Top: For the forward genetic screening, WT yeast strain (CKY457) was UV mutagenized and screened for thiolutin resistant mutants, and mutations were identified by whole-genome sequencing after bulk segregant analysis. Bottom: The gene-specific Variomics libraries consist of many mutants for a given gene in a yeast cell pool, and Variomics libraries for > 4000 genes were further pooled together for thiolutin resistance screening. Plasmids from the validated thiolutin resistant mutants were recovered for Sanger sequencing to identify both the gene and potential mutations. (B) Reproducibly-isolated thiolutin resistant mutants from the forward genetics and manual Variomics screening.(C) Schematic diagram summarizing a partial regulatory network of multiple drug resistance, with isolated resistant mutants indicated. The

reported or hypothesized functional interactions are indicated by pointed (activation) or blunt-end (inhibition) arrows. (D) Distinct thiolutin sensitivity of MDR deficient mutants. *pdr1*Δ and *snq2*Δ are sensitive to thiolutin, whereas other tested MDR deficient strains retain resistance. (E) Schematic diagram summarizing the regulatory network of thioredoxin system in yeast, with isolated resistant mutants indicated. (F) Distinct thiolutin sensitivity of some OSR deficient mutants.

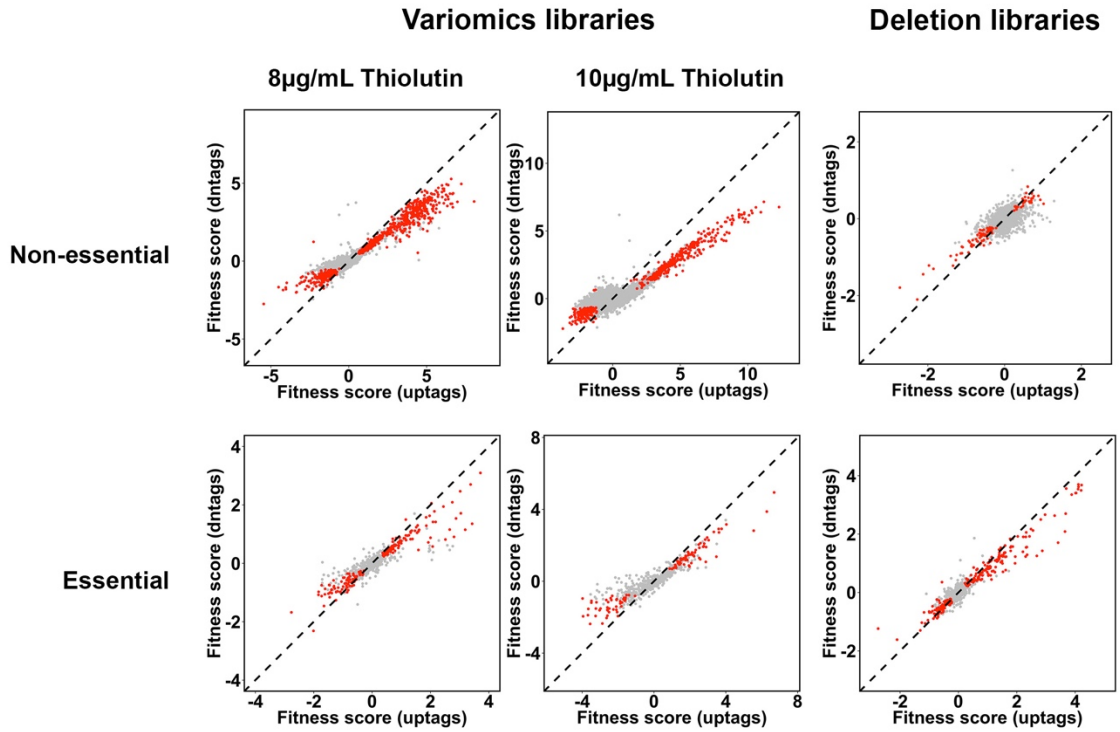

Figure S2. Correlation between uptag and downtags results in Bar-seq. Xyplots showing the fitness score (log2 of the fold change in relative abundance) computed from both uptag and downtags. Mutants are declared significantly resistant or sensitive in both tags are colored in red, whereas others are colored in light grey. y=x is shown as a dashed line.

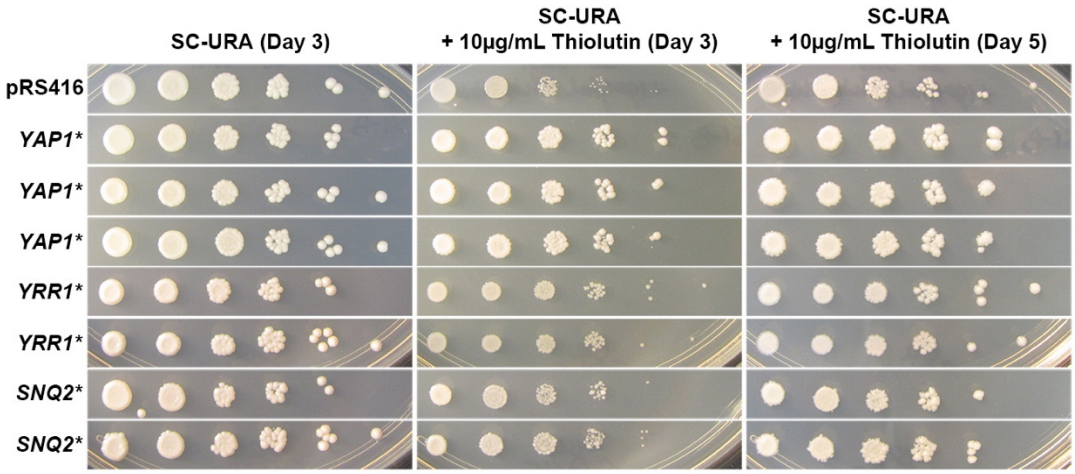

Figure S3. Isolated thiolutin resistant MDR Variomics candidates are dominant or dosage dependent. Plasmids recovered from the Variomics candidates are transformed into WT yeast strain along with an empty vector (pRS416) control, thiolutin resistance are assessed for at least two independent transformants.

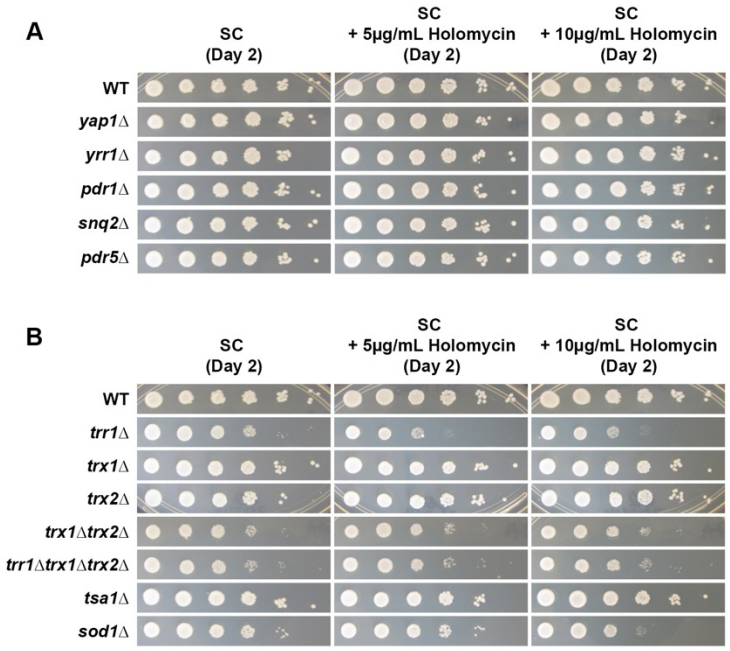

Figure S4. Tested MDR and OSR deficient mutants do not confer the same hypersensitivity to holomycin as to thiolutin.
(A) Plate growth assays of serially diluted MDR deficient mutants on SC complete media with indicated holomycin concentration. (B) Plate growth assays of serially diluted OSR deficient mutants on SC complete media with indicated holomycin concentration.

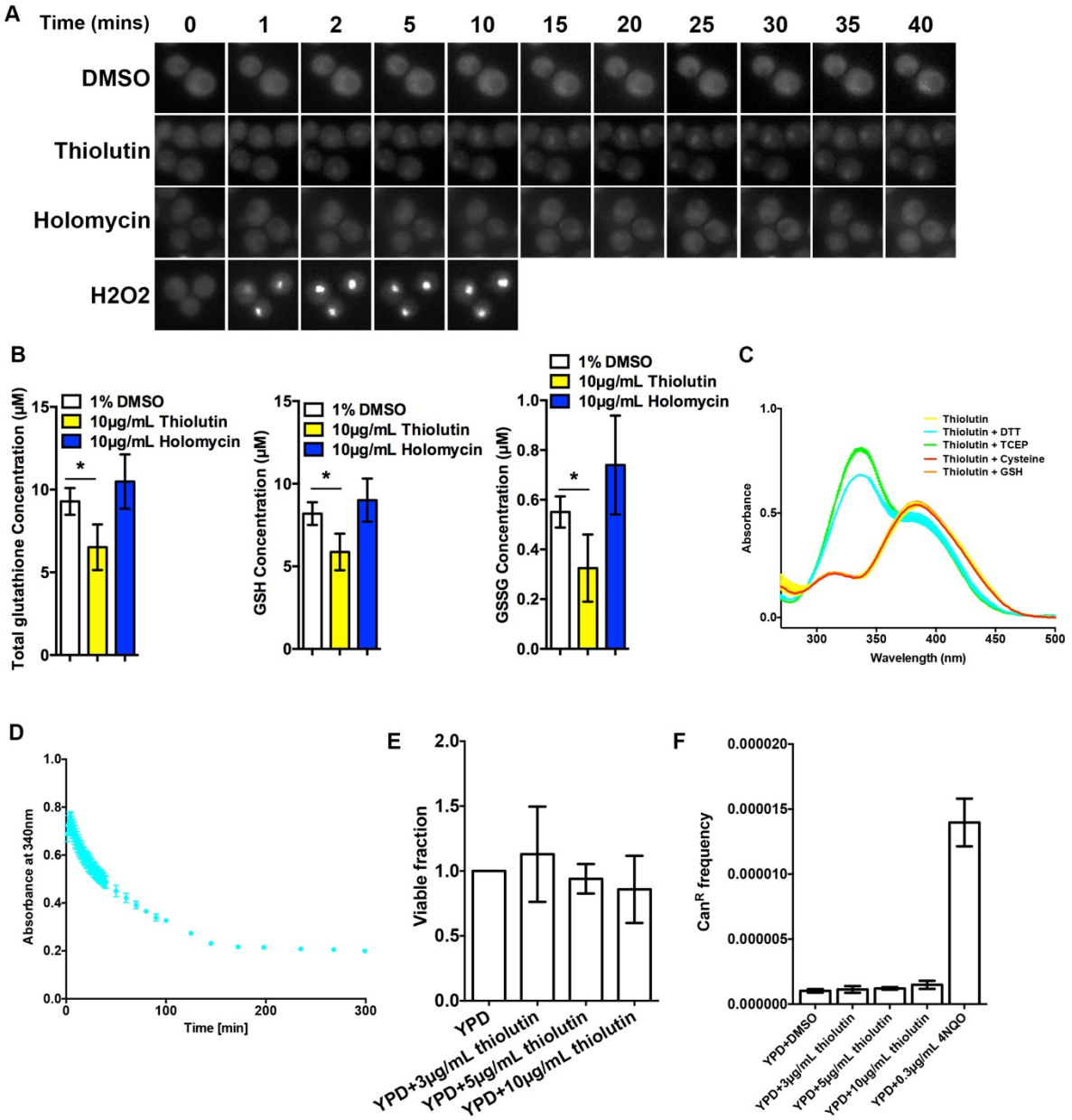

Figure S5. Thiolutin appears to induce oxidative stress partially through redox cycling. (A) Thiolutin induces nuclear localization of the redox-sensitive Yap1 transcription activator. EGFP-tagged Yap1 strain treated with 1% DMSO (control), 10μg/mL thiolutin or 0.4mM H_2O_2. GFP fluorescence was monitored after treatment at the indicated time points. (B) Thiolutin depletes total glutathione *in vivo*. Growing WT yeast cultures are washed and treated with indicated conditions at 30˚C for an hour. Reduced glutathione (GSH) and total glutathione are measured in three independent replicates, and the oxidized glutathione (GSSG) are calculated. The error bars represent standard deviation of the mean. *p≤0.01 (Two-tailed paired t-test). (C) Thiolutin can be reduced by DTT and TCEP, but not glutathione or cysteine *in vitro*. The reactions were performed in 100mM phosphate buffer (pH 6.5) with equivalent molar reductant with thiolutin. UV spectra were measured 1 minute after the reactions. Three independent replicates were performed and the error bars represent standard deviation of the mean. (D) Reduced thiolutin is spontaneously re-oxidized when exposed to air. The reactions were

performed as described in Figure 3D, and UV absorbance at 340nm plotted over a time course. Three independent replicates were performed and the error bars represent standard deviation of the mean. (E) Acute exposure to thiolutin does not affect yeast viability. (F) Thiolutin does not cause DNA damage, as measured by mutation frequency at *CAN1* gene.

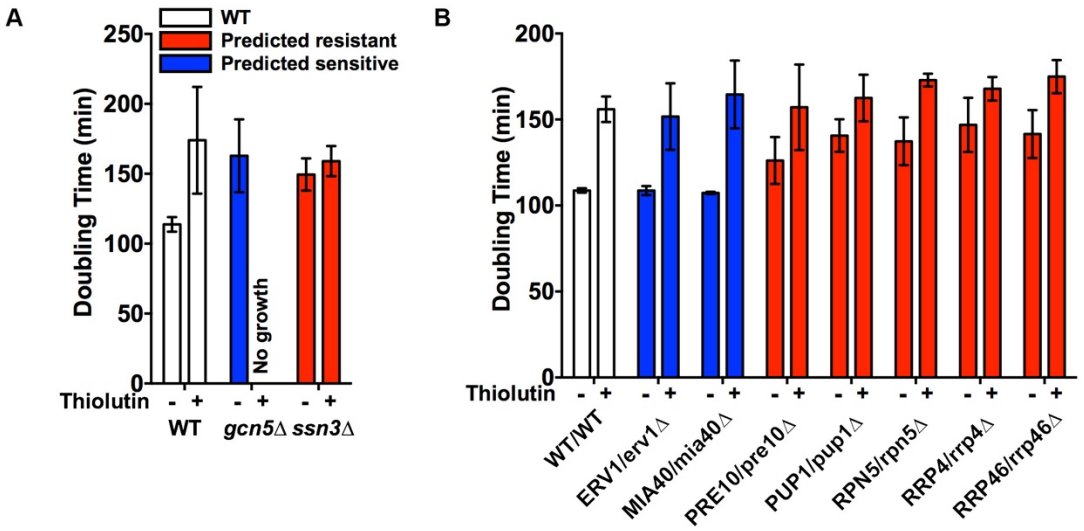

Figure S6. Validation of several statistically significantly resistant or sensitive mutants. Mutants were reconstructed in haploid BY4741 or diploid BY4743 backgrounds originally used to construct the deletion libraries, and mid-log growth at 30˚C was assessed using a Tecan plate reader. Three independent repeats were performed and the error bars represent standard deviation of the mean. We failed to validate the observed slight sensitivity in *ERV1/erv1*Δ and *MIA40/mia40*Δ, two strains that were statistically significantly sensitive in Bar-seq but the sensitivity was very slight.

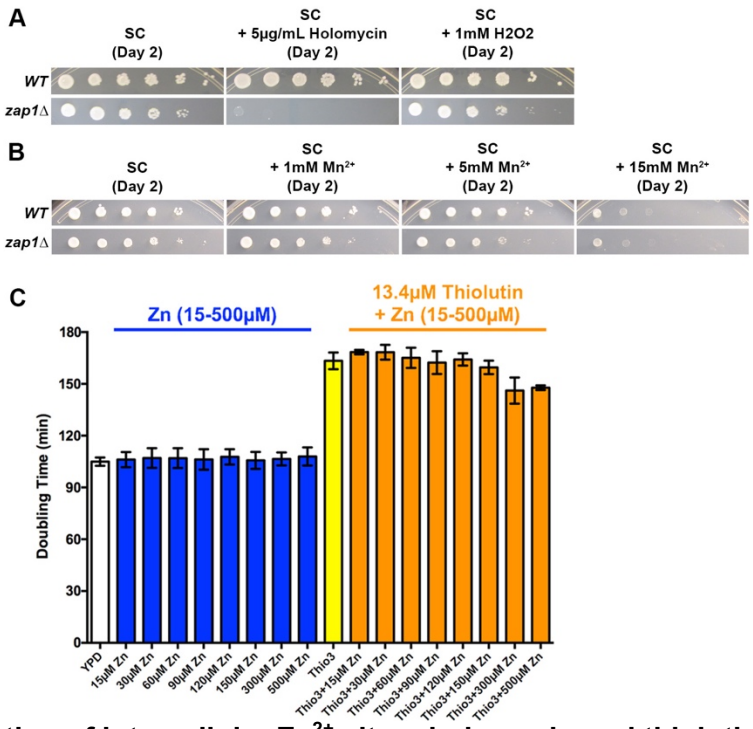

Figure S7. Modulation of intracellular Zn^{2+} alters holomycin and thiolutin sensitivity. (A) *zap1*Δ is hypersensitive to holomycin, but not H_2O_2. (B) *zap1*Δ doesn't confer sensitivity to Mn^{2+}. (C) Zn^{2+} supplementation partially suppresses thiolutin sensitivity. Doubling time were derived from growth curves measured by a Tecan plate reader. Three independent repeats were performed and the error bars represent standard deviation of the mean.

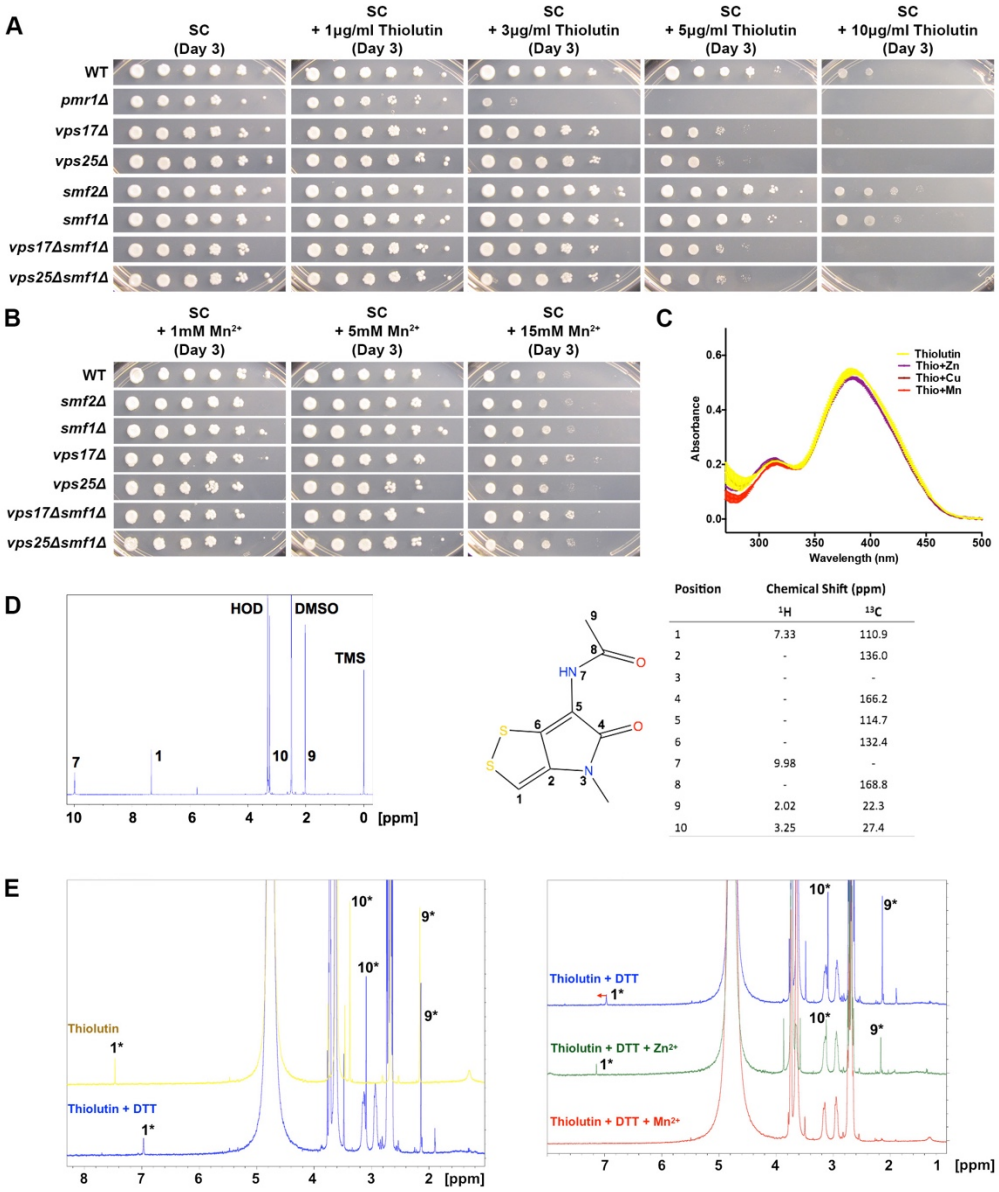

Figure S8. Mn^{2+} may modulate the sensitivity to reduced thiolutin *in vivo* and directly interact with thiolutin *in vitro*.
(A) *pmr1*Δ is hyper sensitive to thiolutin, while *vps17*Δ and *vps25*Δ appear to confer thiolutin sensitivity independent of Smf1-dependent Mn^{2+} trafficking. (B) *vps17*Δ, *vps25*Δ, *smf1*Δ and *smf2*Δ do not confer sensitivity to Mn^{2+} in our strain background and assays. (C) Zn^{2+}, Cu^{2+} and Mn^{2+} do not alter the UV absorbance profile of thiolutin. (D) Assigned 1H-NMR spectrum of thiolutin. (E) Left: Change in thiolutin spectra immediately after reduction by DTT; Right: Changes in DTT-reduced thiolutin chemical shifts after addition of Zn^{2+} (dimagnetic) or Mn^{2+} (paramagnetic).

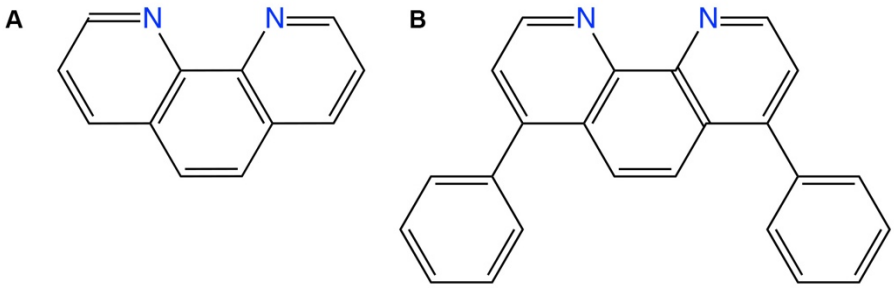

Figure S9. Structures of 1,10-phenanthroline and bathophenanthroline.
(A) 1,10-phenanthroline. (B) bathophenanthroline

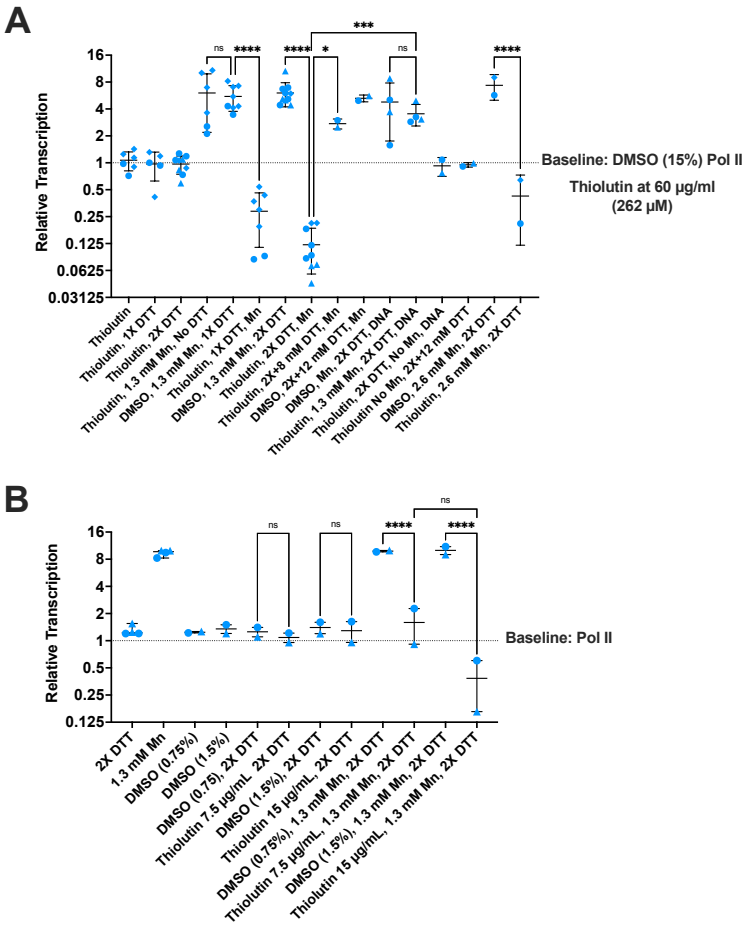

Figure S10. Quantification of thiolutin inhibition under a number of experimental conditions. (A) Thiolutin (60 µg/mL) inhibition of Pol II requires DTT and Mn2+ and is blocked by pre-incubation of Pol II with DNA or with excess (12 mM) DTT added after Pol II treatment with thiolutin. All reactions are compared to baseline for individual Pol II in particular experiment, which is activity of Pol II plus vehicle (15% DMSO final). Different symbols indicate three separate Pol II purifications. Note that variability in fraction of Pol II inhibited by thiolutin appears to track with Pol II purification (▲● Pol II consistently more inhibited than ◆). Error bars are mean +/- Standard Deviation. Statistical analysis for selected pairs is one-way ANOVA with multiple comparisons controlling for False Discovery Rate (0.01) (method of Benjamini, Krieger, Yekutieli). **** = p< 0.0001, *** = p< 0.0002. * p< 0.0332. (B) Quantification of thiolutin inhibition at lower thiolutin/DMSO concentrations and additional controls. All reactions are compared to baseline for individual Pol II in particular experiment, which is activity of Pol II in absence of drug or vehicle. Different symbols indicate two separate Pol II purifications (symbols here match Pol II purifications in (A). Statistical analysis for selected pairs is one-way ANOVA with multiple comparisons controlling for False Discovery Rate (0.01) (method of Benjamini, Krieger, Yekutieli). **** = p< 0.0001.